We are IntechOpen,
the world's leading publisher of
Open Access books
Built by scientists, for scientists

4,800
Open access books available

122,000
International authors and editors

135M
Downloads

Our authors are among the

154
Countries delivered to

TOP 1%
most cited scientists

12.2%
Contributors from top 500 universities

CLARIVATE ANALYTICS

BOOK CITATION INDEX

INDEXED

WEB OF SCIENCE™

Selection of our books indexed in the Book Citation Index
in Web of Science™ Core Collection (BKCI)

Interested in publishing with us?
Contact book.department@intechopen.com

Numbers displayed above are based on latest data collected.
For more information visit www.intechopen.com

Organometallic Materials for Electroluminescent and Photovoltaic Devices

Boris Minaev[1], Xin Li[2,3], Zhijun Ning[2], He Tian[3] and Hans Ågren[2]
[1]Bogdan Khmelnitskij National University
[2]Royal Institute of Technology
[3]East China University of Science and Technology
[1]Ukraine
[2]Sweden
[3]People's Republic of China

1. Introduction

Electroluminescent devices, solar energy conversion technologies and light-emitting electrochemical cells represent a promising branch of modern optoelectronic industry based on organic dyes and polymers as the main working materials. Elementary processes like energy flow through an organic-inorganic interface and voltage control at a molecular level with peculiar electronic properties are now well understood and used in fabrication of new efficient and sophisticated optoelectronic devices. Today, organic light emitting diodes (OLEDs) are used commercially in displays and various lighting applications providing high external quantum efficiency (up to 19%) and low power consumption (Nazeeruddin et al. 2009).

Electroluminescence of organic materials was observed for the first time by Martin Pope et al. (Pope et al. 1963) a half of a century ago. Twenty-four years later the pioneering work of Eastman Kodak Company (Tang & VanSylke 1987) provided the use of 8-hydroxyquinoline aluminum (Alq_3) as electron-transporting and emissive material (Scheme 1) in an OLED device. Since then a growing progress has been witnessed in the field of organic optoelectronics through incorporation of various combinations of organic polymers, dyes and organometallic complexes (Yersin & Finkenzeller 2008, Köhler & Bässler 2009).

Organic conjugated polymers, like poly(para-phenylene vinylene) (PPV) doped by various chromophores, are now used in OLEDs as they lend the possibility to create charge carrier recombination and formation of excitons with high efficiency of light emission. Typical OLEDs are fabricated by spin-coating, inkjet printing or by vacuum deposition of organic materials on an indium-tin-oxide (ITO)-coated glass and with a multilayer structure of the device including NPB (N,N'-Bis(naphthalene-1-yl)-N,N'-bis(phenyl)-benzidine) and Alq_3 as the hole transport layer (HTL) and electron transport layer (ETL), respectively. These materials are presented here as typical examples. In between there is a doped emission layer (EML). Usually some additional layers which protect the ETL from reactions with the cathode material, or reduce the injection barrier and electron-hole quenching, are incorporated into the device architecture. These OLEDs are thin, flexible, stable, and energy

conserving devices; they have prompt response times (μs), high color purity and are suitable for large screen displays and even for illuminating wallpapers in the near future.

In this review we will mostly discuss a new OLED generation with triplet emitters based on cyclometalated transition metal complexes which have attracted extensive attention in the past decade since their external quantum efficiency exceeds that of usual organic materials. In purely organic EML polymers, like PPV or PPP, the energy stored in triplet states cannot be utilized in order to increase the emissive efficiency of OLEDs, since the transition from the lowest triplet (T_1) to the singlet ground (S_0) state is strictly forbidden; this energy thus is mostly spread non-radiatively into backbone phonons and heating of the sample. It has been proposed that that the use of the triplet states may improve an efficiency of solar cells to a large extent (Köhler & Bässler, 2009; Wong, 2008). Singlet state emitters, like Alq_3 (Scheme 1), as a key electron transporter in ETL and new nonmetallic complexes will also be analyzed in this review.

Introducing $Ir(ppy)_3$ in doped EMLs provided a new revolution in modern OLED optoelectronics (Baldo et al. 1999). With the Ir(III) complexes as dopants the electroluminescence is enhanced by harnessing both singlet and triplet excitons after the initial charge recombination, since spin-orbit coupling (SOC), being much stronger in heavy elements like iridium, removes the spin-forbidden character of the singlet-triplet (S-T) transitions. The search for OLED materials was initiated by the classic example $Ru(bpy)_3{}^{2+}$, which was used as a photocatalyst in solar-driven photoconversion processes. The task was to alter the excited state redox potential of similar metal complexes by several modifications; changing the central transition metal, replacing some of the ligands and modifying the ligands by adding suitable functional groups. For example, changing the metal center in $Ru(bpy)_3{}^{2+}$ to Ir(III) produces a complex, $Ir(bpy)_3{}^{3+}$, with excellent photo-oxidizing power. The neutral bpy ligand was changed by the negatively charged ppy. These changes provide a crucial improvement of the chromophore stability and finally became a lucky choice for implementation in modern OLEDs.

Similar problems of the dye optimization are present for the dye-sensitized solar cells (DSSC) based on TiO_2 nanocrystals. They have become of considerable interest as renewable power sources because of the ability to provide a high coefficient of light conversion to electricity (up to 10.4 percent). DSSCs commonly use sensitizers based on complexes of ruthenium with bipyridine (bpy) and other ligands. The most successful example of DSSCs is a Grätzel cell in which the ruthenium(II) bis(4,4'-dicarboxy-2,2'-bipyridyl)-bis(isothiocyanate), denoted by the N_3 dye, is used as sensitizer (Grätzel, 1990); other similar dyes have also served for this purpose. All these organometallic dyes absorb visible light and, being in the excited state, provide electron transfer to TiO_2 crystals on the surface of which they are adsorbed. After that, the oxidized chromophore is reduced by the electrolyte and the cycle is repeated. The requirements to a sensitizing chromophore are universal: high light absorption coefficient in the entire intense solar spectrum, ability to inject an electron into the conduction band of TiO_2, and fast reduction by the electrolyte. The choice and optimization of the chromophore are highly important for the DSSC technology.

To make systematic choices, it is necessary to know the relationship between structures and optical properties of dye molecules. For this purpose, a number of quantum-chemical calculations of electron absorption spectra of the most important sensitizers based on complexes of ruthenium(II) and iridium(III) with polypyridines have been carried out in recent years. Theoretical studies of phosphorescent dopants for OLEDs are of similar

importance. Nowadays, almost all new dyes for DSSCs and OLEDs become subjects for comprehensive photophysical, electrochemical and quantum-chemical density functional theory investigations. The aim of the present review is to describe new synthesis of organometallic complexes based on Ir, Ru, Pt and other ions which are prospects for effective OLEDs and solar cell fabrication and to present the theoretical background that is important for these dyes.

Alq_3 $Ir(ppy)_3$ $Ir(bpy)_3^{3+}$ $Ir(ppy)_2(pic)$
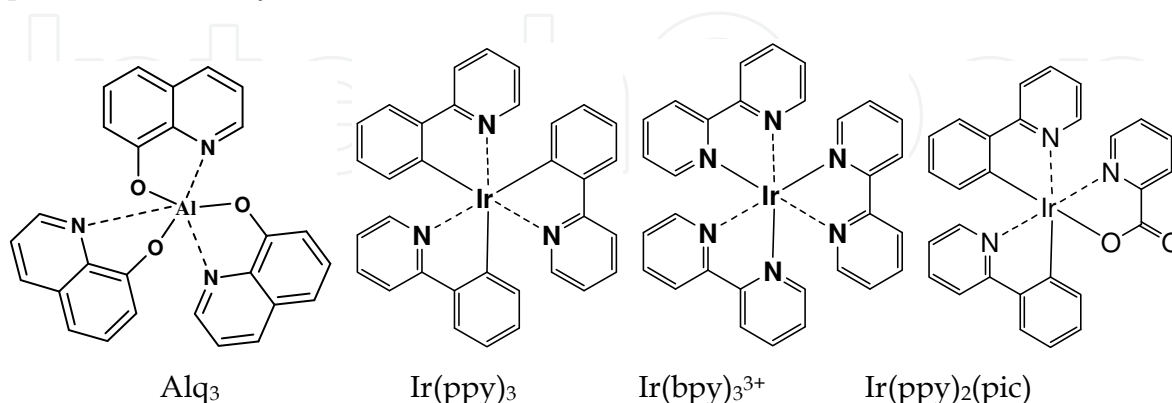
Scheme 1.

We will discuss Ir-complexes of the type shown in Scheme 1, our own synthesized dyes and a number of those which are known from the literature. The main subject of this Review is a theoretical analysis of the structural factors which determine high efficiency of new OLED materials, which we have provided by calculations of various CICs and other dyes. Our unique ab initio calculations of spin-orbit coupling effects and phosphorescent lifetimes in these heavy metal compounds permit us to derive some general ideas about the synthesis of the best phosphorescent sensitizing chromophores for OLEDs and DSSCs.

2. Principles of optoelectronics based on organic materials

2.1 Electroluminescence with low power consumption

OLEDs are based on polymers multi-layer structures. Inside each layer the electronic excitations in the repeating molecular units, being linked by covalent bonds, represent rather complicated excitons. Such excitations in a polymer chain are extended over several molecular links and are associated with the distortion of the polymer. The exciton energy decreases when the size of the excited area increases, but the Coulomb attraction in the electron-hole pair (EHP) can confine the exciton. Principles of electro-luminescence in organic polymers are described in a number of references (e.g. Pope & Swenberg, 1999; Yersin & Finkenzeller, 2008; Köhler & Bässler, 2009). In this review we concentrate our attention on the theoretical description of molecular states at the microscopic level; thus the macroscopic picture of the structural elements of OLEDs and photovoltaic devices will be shortly presented in the form of main concepts of their architecture, connected with organic and inorganic materials in different aggregate states.

Organic materials used in modern optoelectronics can occur in the form of polymer layers, molecular crystals or supramolecular assemblies. Optical characteristics of these materials are intrinsically determined by their molecular properties, which we here will generalize in a simplified manner (Fig. 1). Their conductivity and charge carrier properties are also determined by molecular orbital (MO) properties, but mainly by external perturbations;

injection from the electrodes in the OLED devices or through the dissociation of EHPs created by the incident light in the solar cells, which also require some simple model descriptions. In organic molecular crystals weak van der Waals interaction provides very narrow (≤0.5 eV) valence and conduction bands; in polymers these bands are wider.

In Fig. 1 we present a scheme that illustrates the creation and propagation of excitons in a conjugated polymer chain, which is simulated by four molecular blocks. In real polymers there are thousands of blocks; furthermore, in OLEDs there are few different polymer layers, where the molecular blocks have different MO energy levels. We omit these details for simplicity in Fig. 1.
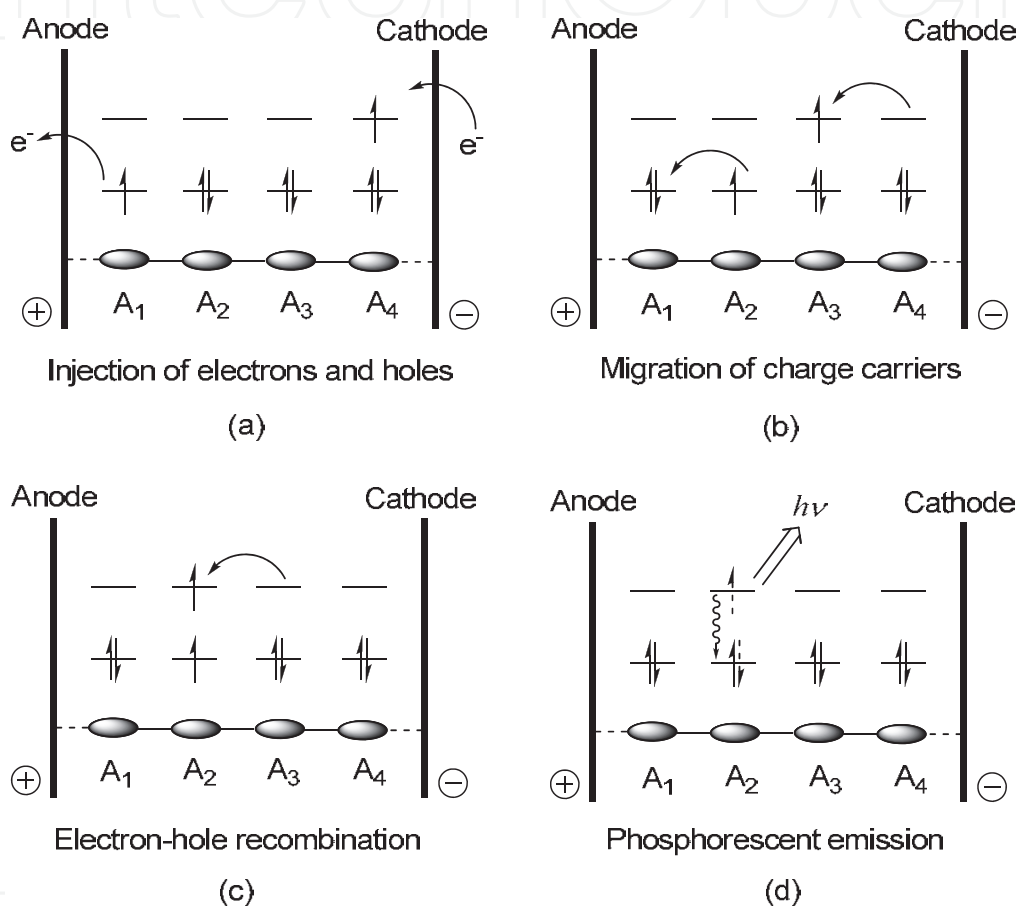

Fig. 1. Scheme of triplet exciton injection and phosphorescent emission in polymer OLEDs

Each molecular block is presented by only two molecular orbitals (MO): the highest occupied MO and the lowest unoccupied MO. Fig. 1 represents the corresponding HOMO and LUMO energy levels in the absence of an electrical bias. Upon voltage application across the electrodes injection of electrons and holes occurs at the cathode and anode, respectively (Fig. 1, a). The molecule A_1 donates an electron to the anode and creates a hole in the polymer, while the molecule A_4 accepts an electron from the cathode. Electrons and holes migrate through the polymer chain in the opposite directions because of the applied voltage; getting closer they start to attract each other until they occur at the neighboring blocks A_2 and A_3 (Fig. 1, b).

The critical radius R_C for the mutual interaction inside the EHP is defined as the distance at which the Coulomb attraction is equal to the thermal energy:

$$kT = e^2 / 4\pi\varepsilon\varepsilon_0 R_C \,, \tag{1}$$

where $\varepsilon, \varepsilon_0$ represent the dielectric constants of the polymer material and the vacuum (Köhler & Bässler, 2009). The low dielectric constant for a typical organic polymer ($\varepsilon = 3$) provides at room temperature quite a big Coulomb capture radius of about 19 nm. In organic polymer films the repeating molecular units (A_n) are linked through covalent chemical bonds and electrons and holes are not strictly localized; in some polymers the charge carrier wave function can extend over several molecular blocks. If we return back to the simple picture in Fig. 1, it is clear that electrons and holes localized at the neighboring blocks A_2 and A_3 have overlapping wave functions. This means a high probability of an electron "jump" from A_3 to A_2, or electrons-hole recombination. After their recombination an electronically excited molecule A_2 is obtained (Fig. 1, c), which can emit light (Fig. 1, d).

In Fig. 1 the triplet state of the electron-hole pair (EHP) is shown, but it can be created in the singlet state as well. Annihilation of the singlet EHP leads to the singlet excited state S_1 of molecule A_2 which can emit light in the spin allowed singlet-singlet transition to the ground state S_0 (Fig. 2). Spontaneous emission $S_1 \rightarrow S_0$ is usually characterized by a short lifetime (ns) because of the large electric dipole transition moment for the spin allowed singlet-singlet transition. This is a typical mechanism of electroluminescence in pure organic light emitting diodes. Radiative rate constants of photofluorescence (k_3) in such polymers is usually a million times larger than those of phosphorescence (k_4), which cannot compete with nonradiative quenching (k_5) in pure organic polymers at room temperature.
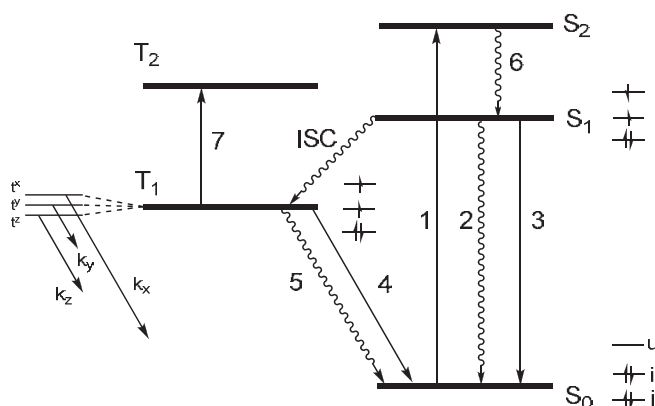

Fig. 2. Main photoprocesses following light absorption by an organic molecule (1). Wavelines - nonradiative quenching; ISC – intersystem crossing; 3 – fluorescence (rate constant $k_3 \sim 10^9$ s^{-1}, radiative lifetime $\tau_3^r = 1/k_3 \approx$ ns); 4 – phosphorescence (k_4 is in the range 0.01-10^6 s^{-1}); 7 – triplet-triplet absorption.

In organic solids solvents, excited state levels are shifted with respect to free molecules in gas phase due to inhomogeneous broadening. In an amorphous film or glass, each molecule has its own particular environment with different orientations and distances to its neighbors. This random variation of electronic polarization of the neighborhood leads to a particular shift of the excited state energy for each molecule (inhomogeneous broadening of spectral lines). For the triplet excited state this broadening is smaller than for the singlets, because electron correlation is stronger for the former (Pope& Swenberg, 1999).

Modern OLEDs often contain an organic polymer in the emission layer doped by a transition-metal complex with heavy iridium or platinum ions, which provide a strong SOC

that makes the $T_1 \rightarrow S_0$ transition to be effectively allowed ($k_4 \sim 10^6$ s^{-1}). In this case the triplet excitons also produce useful work in the OLED (Fig. 1, d). Dopants in EMLs not only collect the S and T excitons by the EHP recombination, but can also be used for regulation of the OLED color. In particular, iridium complexes, containing large π-conjugated ligands (Scheme 1), such as 2-phenylpyridine anions (ppy$^-$) and neutral 2,2'-bipyridines (bpy), have the advantage that their emission wavelength can be tuned from blue to red by peripheral substitution in the rings by electron-withdrawing and electron-donating substituents or by replacement of chelating ligands. The S_1-T_1 splitting (Fig. 2) is determined by the double exchange integral, $2K_{i\text{-}u}$, for φ_i and φ_u orbitals (typically HOMO and LUMO)

$$K_{i-u} = \iint \varphi_i(1)\varphi_u(1)(e^2/r_{1,2})\varphi_i(2)\varphi_u(2)dv_1 dv_2 \,, \tag{2}$$

which is large for the π-π^* states of conjugated molecules (about 1 eV); for the σ-π^* or n-π^* and charge-transfer states the exchange integral is rather small (about 0.1 eV); numbers in brackets (1) and (2) denote coordinates of two electrons in Eq. (2), $r_{1,2}$ is the interelectron distance.

The rate of intersystem crossing in most conjugated molecules and polymers is apparently very low with some exceptions like fullerene and anthracene. Deuteration of organic molecules often suppresses the k_5 rate; the C-H vibrational frequency is much higher than that of the C-D bond vibration and higher overtones should be excited in the deuterated species in order to accept the excess energy $E(T_1)$-$E(S_0)$ and transfer it into vibrational relaxation. From this example one can realize that the nonradiative energy transfer is determined by electron-vibrational (vibronic) interaction to a large extent. This notion can also be applied to the electron-hole injection, migration and recombination processes, and electron transfer in DSSCs (Minaev et al, 2009b).

Since ISC is a spin-forbidden T-S quantum transition, its rate constant also depends on SOC, and on the relative positions of nearby electronic and vibronic states of different symmetry and spin-vibronic interactions (Minaev & Ågren, 2006). Calculations of SOC and radiative rate constants are very important for understanding the function of modern OLEDs. This will be considered in next chapter with explanation of the left part in Fig. 2, where the splitting of spin sublevels of the T_1 state is exaggerated.

Here we need to elucidate some principles of electron-hole migration in more detail. Organic semiconductors have low conductance due to disorder in the amorphous or polycrystalline body; electron and hole mobilities are typically 10^{-8} - 10^{-3} cm^2/V s. In contrast, the perfect molecular single crystal of pentacene has a hole mobility as large as 1.5 cm^2/V s at room temperature (Köhler & Bässler, 2009). All these organic materials have very narrow conduction and valence bands (CVBs), since the molecules are weakly bound by van der Waals interactions. Narrow CVBs imply a mean scattering length of charge carriers to be comparable with intermolecular distances (0.4 nm). Photoexcitation creates predominantly the excited state on an individual molecule (Fig. 2) in such a crystal. Because of translational invariance this excited state may likely reside on any neighboring molecular block in the crystal. It can move through the crystal and is treated as a quasiparticle (exciton). In polymers the exciton wave function can extend over two molecules depending on geometry distortion of the excited state in the chain (charge-transfer exciton). In π-conjugated polymers, like PPV, the electron-hole distance is about 1 nm in the singlet state and about 0.7 nm in the triplet state (Köhler & Bässler, 2009). The difference is determined by exchange interaction of the type presented in Eq. (2). The notations of molecular orbitals (i, u) can refer to HOMO and LUMO inside one molecule, or to different molecules (even to different

polymer chains in the case of an inter-chain exciton). The total wave function may be presented in a general form which includes charge-transfer and local molecular excitations:

$$\Psi = c_1 \Psi(A^- B^+) + c_2 \Psi(A^+ B^-) + c_3 \Psi(A * B) + c_4 \Psi(AB*),$$ (3)

where A and B refer to different polymer blocks, A* indicates the excited A molecule. If the ionic terms dominate $(c_1, c_2 >> c_3 c_4)$ the wave function in Eq. (3) describes a charge-transfer exciton. The opposite case $(c_1, c_2 << c_3 c_4)$ corresponds to an exciplex or an excimer. For an excimer the two molecules are the same (A=B) and this is a model for a Frenkel exciton in molecular crystals. In OLEDs the excited states are formed by recombination of two injected charges in EHP ($c_2 \approx 0.99$ in Eq. (3) and A$^+$ = A$_2$, B$^-$ = A$_3$ in Fig. 1, b). If the positive and negative charges on two molecules are bound by Coulombic interaction one can speak about a geminate polaron pair. For real polymers all coefficients in Eq. (3) are nonzero and their ratio depends on the the A-B distance.

2.2 Solar energy conversion
The mechanism of electric power generation in solar cells is opposite to the mechanism of OLED operation, presented in Fig. 1. The incident light produces an electronic excitation of a dye unit or of a polymer/inorganic crystal followed by charge separation with the subsequent need for the EHP to reach some heterojunction. In solar cells based on crystalline silicon an exciton is created by photoexcitation in one material and the singlet (or triplet) excited state diffuses to the interface with the other material, where dissociation to an electron and a hole takes place. If the energy gained exceeds the exciton binding energy, and if the percolation path for the separated charges affords them to reach the respective electrodes, a voltage occurs. Similar principles of bulk heterojunctions are used in organic semiconductors, when two solutions of polymers with different electronegativity are mixed and spinned on a film (Köhler et al, 1994). The morphology of the film can be optimized by the annealing conditions and the choice of solvent. Solar cells operating both with the singlet and triplet excited states (like in Fig. 1, d) are known. The triplet excitons have longer diffusion length compared to the singlets and this could be used as advantage for such organic solar cells. Despite of the slow Dexter mechanism for the triplet exciton transfer (Forrest, 2004), the large lifetime provides a triplet diffusion length ranging to 140 nm in amorphose organic films, while for singlet excitons it is typically in the range 10-20 nm (Köhler et al, 1994). Polymer-based solar cells operating by triplet excitons also have some advantages, like the triplet emitters in OLEDs, but with completely different physical origin. Inorganic semiconductors, like crystalline silicon, have wider valence and conductive bands than organic solids and also larger dielectric constants ε_r (in silicon ε_r =12, in anthracene ε_r =3). A wide band implies that the mean scattering length of the charge carriers is much larger than the lattice site and exceeds the capture radius R_C of Coulombic attraction for an electron-hole pair (EHP). When an incident light creates an EHP, both charge carriers are delocalized in their wide bands and are not bound by Coulomb attraction. Any scattering event occurs at some distance outside the Coulomb capture radius, R_C, thus the created charge carriers are free in the valence and conduction bands (Köhler & Bässler, 2009). As they are independent of each other, the mutual orientation of their spins is arbitrary; the singlet and triplet states in such EHPs are degenerate, since there is no overlap between the electron and hole wave functions and their exchange energy is zero. This situation for the

spin dynamics is similar to that earlier considered in organic chemical reactions of radicals in solvents. At room temperature the excitons in crystallin silicon are similar to separating radical pairs in the solvent cage. At low temperature, the capture radius R_c in Eq. (1) increases and the EHP bound by Coulomb attraction can exist as a Wannier-type exciton. The binding energy of Wannier excitons in silicon is only 1.42 kJ/mol and the electron-hole separation is about 50 Å (Köhler & Bässler, 2009). The exchange integral, Eq. (2), at this distance is of the order 0.1 kJ/mol, so the S-T splitting of Wannier excitons is marginal. In silicon crystals the exciton wave function, Eq. (3), is presented by the first term $c_2 \approx 0.99$ and the Si atoms are bound by σ-bonds inside the A and B moieties. The direct SOC matrix element between such S and T excitons is equal to zero, since their spatial wave functions are identical; but one-center SOC integrals can contribute in the second order through SOC mixing with the intermediate σσ* states. Since the S-T mixing of excitons is an important problem for both OLEDs and solar cells we will consider here spin-dependent exciton recombination, light emission and other photophysical phenomena starting with spin statistics of a geminate radical pair.

2.3 Spin dynamics in organic solvents and its relation to OLED excitons

Interest in spin-statistics problems in organic chemistry was initiated during studies of radical recombination reactions and chemically induced dynamic nuclear polarization (CIDNP) (Salikhov et al, 1984). CIDNP was detected as a non-equilibrium absorption intensity and emission in NMR spectra of radical recombination products in organic chemical reactions in solvents. It was recognized that the radical pair in the triplet spin state cannot recombine and that it dissociates after the first collision in the cage of a solvent. Only the singlet state pair can recombine and produce a product. After the first collision the triplet radical pair (RP) has a large probability for a new reencounter in the solvent cage. Between the two collisions the separated radical pair can provide a triplet-singlet (T-S) transition and then produce a product of recombination, which is enriched by the nuclei with a particular nuclear spin orientation. The T-S transition is induced by hyperfine interactions (HFI) between the magnetic moment of an unpaired electron in the radical and the particular magnetic moment of the nearby nucleus. The HFI provides a "torque" that promotes the electron spin flip in one radical, which means that a T-S transition takes place in the RP. This, the most popular RP mechanism of CIDNP, has also been applied to chemically induced dynamic electron polarization (CIDEP) in EPR spectra of radical products in photochemistry as well as to magnetic field effects (MFE) in chemistry (Salikhov et al, 1984; Hayashi & Sakaguchi, 2005). In non-geminate radical pairs, produced from different precursors, all possible spin states are equally probable. There are three triplet sub-states and one singlet for each RP; by statistics the number of non-reactive triplet collisions is three times larger than the number of reactive singlets. Thus the T-S transitions in the separated RP between reencounter sequences can increase the rate and the yield of the radical recombination reaction in the solvent. The splitting of triplet sublevels and the rate of the T-S transitions depends on the external magnetic field and this is the reason for MFE in radical reactions. The radical-triplet pair mechanism was later developed for explaining the MFE in radical-triplet interactions. It takes into account MFE for the quartet and doublet states mixing in such interactions. This mechanism has to be used for the treatment of the polaron-triplet annihilation, which is now considered as a reason for triplet state quenching by charge carriers in OLEDs (Köhler & Bässler, 2009).

Similar ideas have to be applied for electron-hole recombination in OLEDs in order to compel the triplet excitons to do useful work in electroluminescent devices. The Wannier excitons are quite similar to the separated radical pairs in the solvent cage if comparison with the CIDNP theory is relevant. Unfortunately CIDEP and MFE theories were not utilized in OLED technology during long time until the first application of the triplet emitters in doped polymers (Baldo et al, 1999), and magnetic field effects are still not used in electroluminescent applications for electron-hole recombination, though it could have some technological applications in organic polymers. The T_1 sublevels are usually depopulated with different rates (k_i, $i = x,y,z$, Fig. 2). In 1979, Steiner reported MFE due to the depopulation type triplet mechanism (d-type TM) on the radical yield of electron transfer reactions between a triplet-excited cationic dye ($^3A^{+*}$) and Br-substituted anilines (D) in methanol at 300 K (Hayashi & Sakaguchi, 2005). Steiner proposed that a triplet exciplex $^3(A^*D^+)$ is generated by charge transfer in this reaction and that the sublevel-selective depopulation is induced by strong SOC at a heavy Br atom during decomposition $^3(A^*D^+)$ = A• + D•+. Similar reactions with triplet exciplexes were found to produce CIDEP and MFE due to d-type TM. The corresponding theory of magnetic field effects due to spin-orbit coupling in transient intermediates and d-type TM has been proposed (Hayashi & Sakaguchi, 2005; Serebrennikov & Minaev, 1987). Its application for charge-transfer excitons in phosphorescent OLEDs is ongoing. First we need to consider the main elementary processes, which occur within the close vicinity of the emitting center in the polymer layer, but general principles of the charge carrier migration and their spin statistics are also discussed.

2.4 Spin statistics of excitons in OLEDs and spin-dependent optoelectronics

As shown in Fig. 1, organic-conjugated polymers are used in OLEDs as they lend the possibility to create charge carrier recombination and formation of excitons with high efficiency of light emission. The typical OLED device consists of a layer of a luminescent organic polymer sandwiched between two metal electrodes. Electrons and holes are first injected from the electrodes into the polymer layer. These charge carriers migrate through the organic layer and form excitons when non-geminate pairs of oppositely charged polarons capture each other. The colliding charge pairs origin from different sources, so they have random spin orientation. Thus the singlet and triplet colliding pairs are equally probable. According to statistical arguments the excitons are created in an approximate 1:3 ratio of singlet to triplet. Fluorescence occurs from the singlet states, whereas the triplets are non-emissive in typical organic polymers, which do not contain heavy metal ions. The triplet-singlet ($T_1 - S_0$) transitions in organic polymers are six to eight orders of magnitude weaker than the spin-allowed singlet-singlet ($S_1 - S_0$) fluorescence. The phosphorescence gains the dipole activity through spin-orbit coupling (SOC) perturbation. SOC is very weak in organic polymers because the orbital angular momentum between the π-π^* states of conjugated chromophores is almost quenched. The other reason is that the SOC integrals inside the valence shell of the light atoms are relatively small (for carbon, nitrogen and oxygen atoms they are 30, 73 and 158 cm^{-1}, respectively). These integrals determine the fine-structure splitting of the ^3P_J term into sublevels with different total angular momentum (J). In light atoms such splitting obeys the Lande interval law and can be described in the framework of the Russell-Saunders scheme for the angular momentum summation.

Thus the emission from triplet states of organic chromophores has very low rate constant and cannot compete with non-radiative quenching at room temperature. Consequently, it

has been assumed that the quantum yield has an upper statistical limit of 25 per cent in OLEDs based on pure organic polymers. In order to compel the triplet excitons to emit light and to do useful work in OLEDs one needs to incorporate special organometallic dyes containing heavy transition-metals into the organic polymers, which will participate in the charge carrier recombination and provide strong SOC in order to overcome spin prohibition of the T_1 - S_0 transition. Incorporation of $Ir(ppy)_3$ into a polymer leads to an attractive OLED material by two reasons: the high rate of electron-hole recombination on the $Ir(ppy)_3$ dye and relatively strong SOC at the transition-metal center induces a highly competitive T_1 - S_0 transition probability and quantum efficiency of the OLED. The cyclometalated photocatalytic complexes of the Ir(III) ion fit these conditions quite well. Involvement of such a heavy atom into metal-to-ligand charge transfer (MLCT) states of different symmetries increases configuration interaction between them and the π-π^* states of the ligands, which finally leads to a strong singlet-triplet SOC mixing in the cyclometalated Ir complexes.

While the ppy ligands are structurally similar to bipyridines, it has been earlier recognized that the metal-carbon bonds which they form with transition-metal ions provide a specific influence on their complex properties that are quite distinct from those of the N-coordinated bpy analogues. Replacing bpy in $Ir(bpy)_3^{3+}$ by 2-phenylpyridine produces a very strong photoreductant, $Ir(ppy)_3$. The enhanced photo-reducing potential of such complexes is attributed to the increase in electron density around the metal due to the stronger donor character of the coordinating carbon atoms. Species containing both bpy and ppy ligands, such as $[Ir(ppy)_2bpy]^+$, have intermediate photoredox properties and can operate as either photo-oxidants or photoreductants. Use of cationic complexes in OLEDs provides some advantages since they do not require complicated fabrication of multilayer structure for charge injection and recombination, which is promising for large-area lighting applications (De Angelis et al. 2007). The presence of mobile cations and negative counter-anions (PF_6^-) makes the ionic complexes more efficient than the neutral cyclometalated iridium complexes (CIC). The ions create high electric fields at the electrode interfaces, which enhances the electron and hole injection into the polymer and also the exciton formation at the dopant metal complexes. Electrons and holes are injected at a voltage just exceeding the potential to overcome the HOMO-LUMO energy gap in the active material of the OLED, irrespective of the energy levels of the electrodes.

The SOC effects on the T_1 - S_0 transition in the $[Ir(ppy)_2(bpy)]^+$ (PF_6^-) and other ionic and neutral iridium complexes have been theoretically studied in order to interpret the high efficiency of the corresponding OLED materials (Minaev et al. 2006; Jansson et al, 2007; Minaev et al. 2009; Baranoff et al. 2010). This affords to foresee new structure-property relations that can guide an improved design of organic light-emitting diodes based on phosphorescence. Modern density functional theory (DFT) permits to calculate the optical phosphorescence properties of such complexes because of their fundamental significance for OLED applications. First principle theoretical analysis of phosphorescence of organometallic compounds has recently become a realistic task with the use of the quadratic response (QR) technique in the framework of the time-dependent density functional theory (TD DFT) approach. These DFT calculations with quadratic response explain a large increase in radiative phosphorescence lifetime when going from the neutral $Ir(ppy)3$ to cationic $[Ir(bpy)_3]^{3+}$ compounds and other trends in the spectra of tris-iridium(III) complexes. Calculations show the reason that some mixed cationic dyes consecutively improve their T_1 - S_0 transition probabilities and unravel the balance of factors governing the quantum emission efficiency in the corresponding organic light-emitting devices.

In order to present connections between main features of electronic structures and photophysical properties including phosphorescence efficiency and energy transfer mechanisms we have to consider spin properties and the SOC effect in atoms and molecules in detail. Since the SOC description in atoms and the multiplet splitting in the framework of the Russell-Saunders scheme is a crucial subject for the new OLED generation of triplet-type emitters, we will pay proper attention to atomic and molecular SOC with special attention to the Ir atom and CIC spectra.

2.5 Spin-orbit coupling

The electron spin wave function Ψ satisfies the equation for the spin square operator of: $\vec{s}^2\Psi = s(s+1)\hbar^2\Psi$, where $s = 1/2$ is a spin quantum number, $\hbar = (h/2)\pi$ is the Planck constant. Two types of spin wave functions Ψ which satisfy this requirement (α, β) and all components of the spin operator are:

$$\alpha = \begin{pmatrix} 1 \\ 0 \end{pmatrix}, \beta = \begin{pmatrix} 0 \\ 1 \end{pmatrix}; s_x = \frac{\hbar}{2}\begin{pmatrix} 0 & 1 \\ 1 & 0 \end{pmatrix}, s_y = \frac{i\hbar}{2}\begin{pmatrix} 0 & 1 \\ -1 & 0 \end{pmatrix}, s_z = \frac{\hbar}{2}\begin{pmatrix} 1 & 0 \\ 0 & -1 \end{pmatrix} \tag{4}$$

Spin was first postulated in order to explain the fine structure of atomic spectra and formulated by Pauli in matrix form, Eq. (4); then it was derived by Dirac in the relativistic quantum theory. In many-electron systems – atoms, molecules, polymers – the electron spins are added by quantum rules into the total spin $\vec{S} = \sum_i \vec{s}_i$, which plays an important role as a fundamental conservation law

$$\vec{S}^2\Psi = S(S+1)\hbar^2\Psi \tag{5}$$

For the even number of electrons the total spin quantum number can be equal $S = 0$ (singlet state), $S = 1$ (triplet state), $S = 2$ (quintet state), which are the most important states in organic chemistry and quantum theory of OLEDs. For odd number of electrons (holes, radicals) the total spin quantum number is usually equal $S = 1/2$ as for one electron, but excited states could have high spin quartet ($S = 3/2$) and sextet ($S = 5/2$) spin. Multiplicity in general is equal to $2S + 1$, which determines a number of spin sublevels in an external magnetic field.

Before calculation of efficiency of triplet emitters in OLEDs one has to analyze quantization of the orbital angular momentum $\vec{L}$ in atoms, which is determined by quantum number L; it needs to be added to spin in order to determine the total angular momentum of atom $\vec{J}$:

$$\vec{L}^2\Psi = L(L+1)\hbar^2\Psi \qquad \vec{J}^2\Psi = J(J+1)\hbar^2\Psi, \text{ where } \vec{J} = L + \vec{S} \tag{6}$$

In relativistic theory all atomic states with L ≠ 0 acquire additional correction to the total energy which is equal to the expectation value of the SOC operator; thus a splitting of atomic terms with different J occurs. Calculation of fine structure is easy to illustrate for a one-electron atom. The SOC operator for the hydrogen-like atom with nuclear charge Z is obtained by Dirac:

$$H_{so} = \frac{e^2\hbar^2}{2\text{m}^2c^2}\frac{Z}{r^3}\vec{l}\vec{s} \tag{7}$$

The operators $\vec{l}\vec{s}$ here are given in $\hbar$ units. The scalar product of two operators $\vec{l}\vec{s}$ can easily be calculated by the definition $\vec{J}^2 = (\vec{L} + \vec{S})^2 = \vec{L}^2 + 2\vec{L}\vec{S} + \vec{S}^2$ with account of Eqs. (5) - (6), which applies also to the single electron case:

$$\vec{L}\vec{S} = \frac{1}{2}[J(J+1) - L(L+1) - S(S+1)] \tag{8}$$

A simple generalization of the SOC operator for a many-electron atom can be summarized in the forms:

$$H_{so} = \zeta \sum_i \vec{l}_i \vec{s}_i = \lambda \vec{L}\vec{S} \text{, where } \lambda = \pm \frac{\zeta}{2S}, \ \zeta_{np} = \frac{e^2\hbar^2}{2m^2c^2}\left\langle \frac{Z}{r^3} \right\rangle_{np} \tag{9}$$

In Eq. (9) Z is a semi-empirical parameter; the "plus" sign corresponds to the open shell, which is "less-than-half" occupied, "minus" – to the "more-than-half" occupied open shell. Using this semi-empirical constant one can calculate SOC in organic molecules. The Ir(III) ion has a $(5d)^6$ configuration: thus its ground state is a quintet ^5D which is split in five sublevels. According to the third Hund's rule the lowest one is $^5D_4$ since the open shell $(5d)^6$ is "more-than-half" occupied and the "minus" sign is used in Eq. (9); thus λ is negative in this case. The maximum J=4 provides SOC energy 4λ, next levels with J=3 has zero correction, and J=2,1 and 0 have positive SOC corrections -3λ, -5λ and -6λ, respectively. The Ir(III) ion is a rather difficult example of SOC treatment in atoms (Koseki at el. 2001). In the neutral Ir atom the ground state 1^4F $(5d)^7(6s)^2$ splitting is more complicated because of non-diagonal SOC mixing with the excited configuration 2^4F $(5d)^8(6s)^1$. In our SOC calculations of iridium complexes we use effective core potential (ECP) and basis set for the Ir atom, augmented with a set of f polarization functions, proposed in Refs. (Cundari & Stevens, 1993; Koseki at el. 2001). The valence orbitals of this ECP are already adjusted for relativistic contractions and expansions, but 5d AOs are nodeless (even though they should have two inner nodes). Instead of the full Breit-Pauli operator (Ågren et al. 1996) we use for the CIC and Pt compounds an effective one-electron SOC operator with effective nuclear charge for each atom A (Koseki at el. 1998)

$$H_{so} = \frac{e^2\hbar^2}{2m^2c^2} \sum_i \sum_A \frac{Z_{eff}(A)}{r_{iA}^3} \vec{l}_{iA}\vec{s}_i \tag{10}$$

This operator was widely used for SOC calculations in molecules and charge-transfer complexes with semi-empirical self-consistent field (SCF) configuration interaction (CI) methods (Minaev & Terpugova, 1969; Minaev, 1972; Minaev, 1978) and also in ab initio approaches (Koseki at el. 1998). For the ECP basis set in heavy elements the effective nuclear charge in Eq. (10) loses its physical meaning and becomes a rather large fitted parameter, since the 5d AO is nodeless. Koseki at el. have obtained $Z_{eff}(Ir) =1150.38$, $Z_{eff}(Pt) =1176.24$. For the first row transition metals and for the lighter elements these parameters have the usual meaning and are close to the values found earlier (Minaev & Terpugova, 1969), since the 3d and 2p functions lack nodes. Multiconfiguration (MC) SCF method with account of second order CI and SOC (Koseki at el. 1998) provides moderate agreement with the observed spectra of Ir and Pt atoms. For the ground state of the Pt atom ^3D $(5d)^9(6s)^1$ the MC SCF + SOCI calculations predict negative excitation energy to the excited ^1S $(5d)^{10}$ configuration which leads to disagreement with experiment when SOC is included in the CI

matrix (Minaev & Ågren, 1999). A multi-reference (MR) CI + SOC calculation improves the results (Table 1). The SOC-induced splitting of the ^3D_J sub-levels deviates rather much from the Lande interval rule but is semiquantitatively reproduced by MRCI+SOC calculations (Table 1) with the parameter $Z_{eff}(Pt) = 1312$ (Minaev & Ågren, 1999). One needs to stress that the experimental S-T energy gap between the $^3D_3$ and $^1S_0$ states (6140 cm^{-1} =0.76 eV) is very far from non-relativistic CI results (0.03 eV) and is determined mostly by SOC. That is why many attempts to reproduce this S-T gap in non-relativistic CI methods have failed (Minaev & Ågren, 1999). This is in a large contrast to the Pd atom with the ^1S $(5d)^{10}$ ground state, where the S-T energy gap is well reproduced in simple CI calculations.

Account of $^3F_4$ $(5d)^8(6s)^2$ state does not influence the old results (Minaev & Ågren, 1999) because the ^3F state energy is rather large in MRCI calculations. But the $^1D_2$ singlet state strongly interacts with the $^3D_2$ and $^3F_2$ triplets, which leads to a low-lying level with J=2. A study of the Pt complexes used in OLEDs indicates that ligand fields strongly influence the S-T energy gap and SOC splitting of the multiplets. The orbital angular momentum of the Pt atom is almost quenched by ligands such as porphine and acetylides (Minaev at el. 2006/a,b) and the zero-field splitting (ZFS) is strongly reduced. ZFS can be reliably estimated by second order perturbation theory, and depends on the square of the SOC matrix elements. The S-T mixing is determined by first order perturbation theory and it is still large in Pt complexes used in OLED; thus the SOC-induced by the Pt atom strongly influences the $T_1 \rightarrow S_0$ emission (phosphorescence) rate in platinum acetylides (Minaev at el. 2006.a) and platinum porphyrines (Minaev at el. 2006.b).

State	MRCI	MRCI+SOC	Expim.	Degener.
(configurat.)	a.u.	cm^{-1}	cm^{-1}	
$^3D_3$ $(5d)^9(6s)^1$	-0.823370	0.00	0.00	7
$^3D_2$ $(5d)^9(6s)^1$	-0.823370	2066.54	775.9	5
^1S $(5d)^{10}$	-0.822295	4646.12	6140.0	1
$^3D_1$ $(5d)^9(6s)^1$	-0.823370	11025.067	10132.0	3
$^1D_2$ $(5d)^9(6s)^1$	-0.807364	12471.36	13496.3	5
$^3F_4$ $(5d)^8(6s)^2$	-0.791214	945.32	823.7	9

Table 1. Splitting of the low-lying states in the Pt atom; from Ref. (Minaev & Ågren, 1999) with some additions; -118.0 a.u. should be added to MRCI column.

The treatment of SOC in the iridium atom is also complicated (Koseki at el. 2001). Account of all electrons with the Breit-Pauli SOC operator definitely improves the SOC splitting of the two low-lying ^4F states (Koseki at el. 2001), but the ECP basis set with an effective single-electron operator, Eq. (10), and the $Z_{eff}(Ir)$ value also give reliable results (Koseki at el., 1998). Our calculations with this approximation of SOC and phosphorescence lifetime in cyclometalated iridium complexes, used in OLED emissive layer, provide good agreement with experimental measurements for radiative characteristics. This is important for a comprehensive understanding of the electronic mechanisms in order to formulate chemical requirements for OLED materials.

2.6 Triplet-singlet transitions and zero-field splitting of the triplet state
Spin-orbit coupling can mix the triplet (T) and singlet (S) states in atoms, molecules and solids. Before studying SOC mixing between excitons one has to analyze the electric dipole

operator ($\vec{m} = e\sum_i \vec{r}_i$) and its transition moment $T_1 \rightarrow S_0$ for a typical molecule or cyclometalated complex with a ground S_0 state (Fig. 2). Let us consider first order perturbation theory for the T_1 and S_0 states:

$$\tilde{T}_1^\alpha = T_1^\alpha + \sum_n \frac{\langle S_n | \hat{H}_{SO} | T_1^\alpha \rangle}{E(T_1) - E(S_n)} S_n \ ; \ \tilde{S}_0 = S_0 + \sum_k \frac{\langle T_k^\alpha | \hat{H}_{SO} | S_0 \rangle}{E(S_0) - E(T_k)} T_k^\alpha \tag{11}$$

The perturbed wave function of the first excited triplet state is denoted here as $\tilde{T}_1$; it is mixed with all singlet states S_n wave functions, including the ground state, n=0. In a similar way the ground state perturbed wave function $\tilde{S}_0$ has admixtures of all triplet states, including k=1. The triplet state wave function T_k^α can be represented as a product of the spatial part $^3\Psi_k = \sum^3 A_{i-u,k} {}^3\Phi_{i-u}$ and the spin part t^α. In the TD DFT method the $^3\Phi_{i-u}$ configurations are presented as two-component matrices, which include single excitations above the closed shell of the type: $^3\Theta_{i-u} = \frac{1}{\sqrt{2}}[\varphi_i(1)\varphi_u(2) + \varphi_i(2)\varphi_u(1)]$. Spin functions of the ZFS sub-levels have a general form (Vahtras et al. 2002):

$$t^x = \frac{1}{\sqrt{2}}[\beta(1)\beta(2) - \alpha(1)\alpha(2)] \ ; \ t^y = \frac{i}{\sqrt{2}}[\beta(1)\beta(2) + \alpha(1)\alpha(2)] \ ; \ t^z = \frac{1}{\sqrt{2}}[\alpha(1)\beta(2) + \alpha(2)\beta(1)] \tag{12}$$

In organic π-conjugated molecules the i - u orbitals, HOMO - LUMO, are of π-type. Zero-field splitting in the T_1 state of such molecules and in organic π-conjugated polymers is determined by weak spin-spin coupling, which usually does not exceed 0.1 cm^{-1}. The SOC contribution to ZFS in these cases is negligible; it occurs in the second order of perturbation theory:

$$\left| H_{\alpha\beta} - E\delta_{\alpha\beta} \right| = 0, \quad \alpha, \beta = x, y, z \ , \tag{13}$$

where

$$H_{\alpha\beta} = H_{\alpha\beta}^{(1)} + H_{\alpha\beta}^{(2)} = \langle T_1^\alpha | H_{ss} | T_1^\beta \rangle + \sum_k \sum_{\alpha\beta} \langle T_1^\alpha | H_{so} | {}^\lambda\Psi_k^\beta \rangle \langle {}^\lambda\Psi_k^\alpha | H_{so} | T_1^\beta \rangle / ({}^3E_1 - {}^\lambda E_k) \tag{14}$$

Here $\lambda = 2S + 1$ means multiplicity of the perturbing state. Summation in Eq. (14) includes S=0, 1, 2, that is SOC mixing of the lowest triplet T_1 with all singlet, triplet and quintet states in the spectrum. If the SOC mixing with the triplet state $^3\Psi_k$ produces down-shift of the T_1^x and T_1^y spin-sublevels, then the corresponding singlet state $^3\Psi_k$ produces a similar shift of the $^zT_1$ sub-level. If the T_1 state is of π-π* nature, the perturbing states are of σ-π* (or π-σ*) nature. In this case the S-T splitting $^3E_{\pi\pi*} - {}^1E_{\sigma\pi*}$ and T-T splitting $^3E_{\pi\pi*} - {}^3E_{\sigma\pi*}$ are almost the same. The corresponding SOC integrals between T-T and S-T states are also very similar. Thus the SOC contribution to ZFS from the analogous singlet and triplet counterparts is negligible. It is less than 10^{-5} cm^{-1} in the benzene and naphthalene molecules, thus the ZFS is completely determined by weak spin-spin coupling. One can see that the SOC contribution to ZFS strongly depends on the S-T splitting of the perturbing states. If the lowest triplet is of n-π nature, like in pyrazine or benzoquinone, the perturbing S and T states are of π-π* type. The exchange integral, Eq. (2), for π-π* orbitals is usually rather large, thus one can expect an appreciable SOC contribution, Eq. (14), to ZFS of the T_1(n-π*) state. Similar analysis has been presented for the Ir(ppy)$_3$ complex (Jansson et al. 2006; Yersin &

Finkenzeller, 2008), which shows that the SOC splitting of the ^{3}MLCT state can be relatively large.

Let us use the perturbed states, Eq. (11), in order to calculate the triplet-singlet transition:

$$< \tilde{T}_1^\alpha \mid m_\gamma \mid \tilde{S}_0 > = \sum_n \frac{\langle S_n | \hat{H}_{SO} | T_1^\alpha \rangle^*}{E(T_1) - E(S_n)} < S_n \mid m_\gamma \mid S_0 > + \sum_k \frac{\langle T_k^\alpha | \hat{H}_{SO} | S_0 \rangle}{E(S_0) - E(T_k)} < T_1^\alpha \mid m_\gamma \mid T_k^\alpha >$$

Since SOC integrals are imaginary and hermitian, $\langle S_n | \hat{H}_{SO} | T_1^\alpha \rangle^* = \langle T_1^\alpha | \hat{H}_{SO} | S_n \rangle$, the last equation can be presented in the form

$$< \tilde{T}_1^\alpha \mid m_\gamma \mid \tilde{S}_0 > = \sum_{n(\neq 0)} G_{1,n}^\alpha < S_n \mid m_\gamma \mid S_0 > - \sum_{k(\neq 1)} G_{k,0}^\alpha < T_1^\alpha \mid m_\gamma \mid T_k^\alpha > + G_{1,0}^\alpha (^1 m_{0,0} - {}^3 m_{1,1}), \quad (15)$$

$$G_{k,0}^\alpha = \frac{\langle T_k^\alpha | \hat{H}_{SO} | S_0 \rangle}{E(T_k) - E(S_0)}$$

and $(^1 m_{0,0} - {}^3 m_{1,1})$ is the difference of the permanent dipole moments of the ground singlet state and the lowest triplet state; its contribution to the phosphorescence k_4 rate constant requires special attention and will be analyzed later.

3. Iridium(III) complexes in OLED materials

Iridium as heavy metal center can provide large SOC and therefore allows the spin-forbidden S_0-T_1 transition which facilitates the utilization of triplet emission energy in OLED materials. The first prototype of iridium-containing dyes used in OLED was tris(2-phenylpyridine)iridium, i.e. the Ir(ppy)$_3$ complex, which was found to improve OLED devices. Nowadays iridium complexes constitute an important class of dopants for organic polymers used in OLEDs in order to increase the efficiency of electroluminescence. Iridium complexes have advantages such as strong phosphorescence in the visible region and tunable emission wavelengths through peripheral functionalization of the ligands.

Heteroleptic iridium complexes have advantage that functions of different groups can be integrated into one molecule. Such complexes usually consist of two cyclometalating ligands (C^N) and one ancillary ligand. By changing the functional groups in the ancillary ligand or introducing a novel ancillary ligand, the photophysical properties of the complex can be tuned. For example, fluorine substitutions are often introduced into the ligand in order to lower the HOMO energy level and to obtain a blue-shifted emission wavelength. Interestingly, some iridium complexes containing switching units can respond to external electric or photo stimuli, leading to controllable and modulatable phosphorescence emission.

3.1 Spin-orbit coupling in cyclometalated iridium complexes

Modification of a CIC by modulating ligands for enhancement of their phosphorescence and tuning of its wavelength from blue to green and red colors is an important task for both theoretical and applied research. A theoretical background for the chemical and photophysical properties of transition metal complexes with polypyridyl ligands was developed a long time ago in the framework of crystal field theory and ligand field theory

using quasi-octahedral symmetry (Nazeeruddin at el. 2009). High symmetry of the coordination sphere and relatively weak perturbation of d-AOs of the metal center by a ligand field implies that the orbital angular momentum of the metal ion is not completely quenched in the complex. Though an expectation value of L is zero in polyatomic systems, and Eq. (8) provides zero SOC correction to the nonrelativistic energy, non-diagonal terms of the SOC operators in Eq. (9) and (10) can generate large coefficients $G_{k,n}$ in Eq. (15) and even corrections to the expectation value of L (Minaev, 1978). The Ir atom is in the group VIII B, and lies below Co and Rh. The splitting of d-orbitals is rather specific in this series. The Ir(III) ion is characterized by relatively strong ligand field splitting between the occupied t_{2g} MO group and the unoccupied e_g pair of the 3d orbitals compared to other ions, thus it is easier to tune CIC emission by ligand modulation. Because of the larger nuclear charge of Ir, the SOC splitting and multiplet mixing is much stronger in CIC than in cobalt and rhodium complexes, thus enhanced S-T transitions and ISC is expected in CIC compounds. That is why the efficient quantum yield of the T_1 states and intense phosphorescence distinguish the photophysics of heavy metal complexes from those of organic and light metal compounds.

The photophysics of polypyridyl iridium complexes can be understood accounting for three types of excited state configurations: metal-centered (MC) excited dd* states of the t_{2g} - e_g type, ligand-centered (LC) excited π-π* states, and metal-to-ligand charge transfer (MLCT) states. The TD DFT calculations indicate that the lowest triplet T_1 state is a mixture of the MLCT and LC excited state configurations (Minaev et al. 2006, Minaev et al. 2009, Nozaki 2007). In Ir(ppy)$_3$ the HOMO is a mixture of 5d-AO (t_{2g}) and the phenyl ring π-orbitals, in contrast the LUMO is a pure π*-orbital of the pyridine moiety. In this case the $G_{1,0}$ value (Eq. 17) is negligible because the SOC integral includes a HOMO-LUMO angular momentum matrix element which does not contain one-center integrals at the metal. With this as background one can explain the low rate constant (k_5, Fig. 2) for the $T_1 \sim\rightarrow S_0$ non-radiative quenching of the phosphorescent emission. This is in a general agreement with a high phosphorescence quantum yield (φ_P) of CIC compounds. Some variations in φ_P are explained by SOC calculations of the $G_{1,0}$ coefficient, Eq. (15) (Li et al. 2011).

Analysis of Eq. (15) in the framework of TD DFT quadratic response calculations reveals general reasons for the high radiative rate constant (k_4, Fig. 2) for the $T_1 \rightarrow S_0$ phosphorescent emission. Intensity borrowing from the $T_1 \rightarrow T_k$ electric dipole transitions (last sum in Eq. (15)) provides the largest contribution to the phosphorescence intensity. The metal-centered (MC) excited triplet ^{3}dd* states of the $t_{2g} \rightarrow e_g$ type represent the higher triplets, T_k, which have strong SO coupling with the ground singlet state, S_0, and simultaneously – a large $T_1 \rightarrow T_k$ electric dipole transition moments (last sum in Eq. (15)). The reason is obvious; the $<T_k | H_{so} | S_o>$ matrix elements include one-center SOC integrals at the metal, which are determined by a relatively large ζ_{5d}(Ir) value. The $T_1 \rightarrow T_k$ electric dipole transition moments do not depend on SOC and include transitions between LUMO (pyridine π* MO) and e_g (5d $_{x2-y2}$ and 5d$_{z2}$) orbitals, which are allowed, though they are not intense. Besides, there are LUMO+1 contributions which provide more efficient overlap with 5d-AOs and higher dipole moments. Substitution of ligands can influence HOMO and LUMO energies and their mixing with metal 5d-AOs, thus modulating the phosphorescence lifetime and tuning of its wavelength. A series of TD DFT calculations with SOC treatment by quadratic response provide a very good explanation of emission tuning in various CIC

compounds and illustrate the physical reasons for OLED architecture and design (Li et al., 2011, Minaev et al., 2009, Janson et al., 2007, Nozaki 2007).

3.2 Cationic Ir(III) complexes

It is known that ionic cyclometalated complexes of the type $[Ru(bpy)_3]^{2+}(PF_6^-)_2$ do not need complicated fabrication of multilayer devices for charge injection and recombination (Nazeeruddin et al, 2009). These systems are used now in electrochemical devices, which are promising for large-area lighting. Only a single-layer of such ionic complexes operates at a low voltage and these devices are shown to be rather insensitive to the choice of electrode material, allowing the use of air-stable anodes and cathodes. The presence of mobile ions, which carry two net positive and negative charges makes such ionic materials quite different from the neutral organic semiconductors typically used in OLEDs. Upon application of a voltage the anions and cations move toward the anode and cathode, respectively, creating high electric fields at the electrode interfaces, which enhances charge injection into the polymer layer and exciton formation at the metal complexes (Nazeeruddin et al, 2009).

Unfortunately, the ionic systems provide a low quantum yield compared to the neutral complexes; the reason was established by the recent SOC calculation of ionic CIC (Minaev et al. 2009). Until recently, the majority of ionic chromophores used in the single-layer devices have been Ru-based complexes (Nazeeruddin et al, 2009). They emit light in the orange-red region, while for OLED displays white light is usually needed, which can be obtained by mixing blue with red and green colors. Such systems were synthesized in a form of mixed ligand cationic iridium complexes: the green-blue emitting [Ir(2-phenylpyridine)2(4,4′-dimethyl amino-2,2′-bipyridine](PF6-) complex, labeled as N926, and the [Ir(2,4-difluorophenylpyridine)2 (4,4′-dimethyl amino-2,2′-bipyridine](PF6-) complex, labeled as N969. Both show bright emission with high phosphorescence quantum yield (80-85%) at room temperature in an argon-degassed solution of CH_2Cl_2(Nazeeruddin et al, 2009). TD DFT calculations of these systems together with the pure ionic $[Ir(bpy)_3]^{3+}$ complex (Scheme 1) reveal the nature of the $T_1 \rightarrow S_0$ transition efficiency of the corresponding CICs (Minaev et al. 2009).

The spin density distribution and hyperfine constants in the optimized T_1 excited state of the $[Ir(bpy)_3]^{3+}$ complex indicates the biradical "quinoid" structure in one ligand. In this particular bpy ligand the ring bonds, being parallel to the C-C bridge, are getting shorter and the other bonds are elongated upon $S_0 \rightarrow T_1$ excitation. Thus the lowest T_1 state in the pure ionic $[Ir(bpy)_3]^{3+}$ complex is a local $\pi \rightarrow \pi^*$ excitation in one bipyridine moiety. Because of this the $T_1 \rightarrow S_0$ transition is not intense and the calculated phosphorescence lifetime, τ_p, is relatively large (0.1 ms), in agreement with experiment (0.054 ms). In mixed cationic Ir(III) systems the lifetime is much lower and close to the neutral *fac*-Ir(ppy)3 complex: for the latter dye our theory and measurements provide the same value τ_p = 2 µs (Jansson et al. 2007). Our TD DFT calculations of τ_p include SOC between thousands of S,T states and are rather complicated. Thus a good agreement for both τ_p values seems to be a miracle. But it is not, since for the mixed $[Ir(ppy)_2(bpy)]^+$ complex the calculation (Minaev et al. 2009) provides τ_p = 4.83 µs in a perfect agreement with τ_p measurements in solid glass (4.4-5.2 µs). For N926 complex the calculated and experimental τ_p values are equal to 2.94 and 3.04 µs, respectively. The DFT method also provides an explanation for the high phosphorescence quantum yield; a direct SOC between S_0 and T_1 states is negligible in these systems, which

explains the low rate constant (k_5, Fig. 2) for the T_1 state quenching. This SOC integral enters the last term in Eq. (15). It is not important for the radiative $T_1 \rightarrow S_0$ transition dipole moment, Eq. (15), since there are other big contributions at n=4-6. Tuning of the colors in cationic CICs is explained by the energy shifts of the π*(bpy) LUMO in N926 and by strong HOMO stabilization (Ir-ppy) in the N969 complex upon fluorine introduction (Nazeeruddin et al, 2009).

De Angelis et al. (2007) have reported a combined experimental and theoretical study on cationic Ir(III) complexes for OLED applications. The authors also described a strategy to tune the phosphorescent emission wavelength and to improve the quantum yields by modulating the electronic structures the iridium complexes through selective ligand functionalization. The newly synthesized cationic Ir(III) complex, [Ir(2,4-difluorophenylpyridine)$_2$(4,4′-dimethylamino-2,2′-bipyridine)](PF6) or N969 is observed to exhibit blue-green emission at 463 nm with a high quantum yield of 85% in acetonitrile solution at ambient temperature. DFT and TD DFT calculations with solvent effects taken into account were carried out to characterize the electronic structures of the ground state and the excited states. This work shows the possibility of tuning the electronic structures and the excited-state properties as useful for the design of new iridium(III) emitters with specific characteristics.

Ladouceur et al. (2010) have synthesized a family of other cationic iridium(III) complexes containing 4'-functionalized 5,5'-diaryl-2,2'-bipyridines ligands as triplet emitters for OLEDs. Most of the complexes show intense and long-lived phosphorescent emission in both 2-MeTHF and acetonitrile at 77 K and at ambient temperature. Quantum chemical calculations suggest that the emission arises from an admixture of the ^{3}LLCT (π(ppy) --> π*(bpy*)) and the ^{3}MLCT ($d\pi$(Ir) --> π*(bpy*)) states. TD DFT calculations also provide insight into the origin of the electronic transitions. Moreover, the introduction of the peripheral aryl groups in the bpy* ligand is expected to enhance the shielding of the iridium center and therefore to increase the stability of the device.

Cationic bis-cyclometalated iridium(III) phenanthroline complexes with pendant fluorenyl substituents have been described by Zeng et al. (2009). These complexes consist of two 2-phenylpyridine ligands and one substituted phenanthroline ligand, which provides extended π-conjugation. Single-crystal X-ray diffraction measurements reveal that the iridium center adopts an octahedral coordination structure. Two of the complexes display reversible cyclic voltammetric waves which are assigned to the Ir(III)/Ir(IV) couple. Broad bands are observed in the photoluminescence spectra of all the complexes, corresponding to the mixed ^{3}MLCT and $^3\pi$-π* states. The lifetimes in the microsecond time-scale indicate the phosphorescent character of the luminescence, and it is found that larger conjugation length in the ligand leads to longer lifetime. DFT calculations show that the HOMOs are localized on the iridium center and the benzene rings of the phenylpyridine ligand, while the LUMOs are mainly located on the phenanthroline ligand. The light-emitting cells fabricated through the spin-coating approach exhibit maximal brightness efficiency of 9 cd A^{-1} and show very good stability in air.

3.3 Fluorine substitution in the ligands

Fluorine substitution is usually introduced into CIC to obtain intense blue emission. In the TD DFT study carried out by Li et al. (2011), linear and quadratic response approaches are employed to investigate the absorption and luminescence spectra of several facial and

meridional iridium complexes with fluorine-substituted phenylpyridine ($F_n$ppy) ligands, as shown in Fig. 3. Similar to other Ir(III) complexes, the HOMOs are mainly localized on the metal center and the phenyl ring of the ppy ligands while the LUMOs are delocalized mostly on the pyridine part of the ppy ligands. The computations also suggest that the presence of the fluorine atoms in the ppy ligand will enlarge the HOMO-LUMO energy gap and result in blue-shifted emission. Moreover, the SOC strength and the radiative rate constant are diminished by the introduction of fluorine substitutions. Linear response calculations reveal that the S_0-T_1 SOC matrix element is smaller in the *fac*-isomer than in *mer*-complexes, which means that the nonradiative quenching of the T_1 state is faster in the latter complexes. Therefore in the meridional isomer the SOC matrix element together with the difference between the permanent dipole moments of the T_1 and S_0 states, Eq.(15), provide destructive contribution to the total $S_0 \rightarrow T_1$ transition moment. This study has shown the effects of the fluorine substitutions and the facial to meridional isomerization to the photophysical properties of the iridium complexes.

Avilov et al. (2007) have studied a series of Ir(III)-based heteroleptic complexes with phenylpyridine (*ppy*) and 2-(5-phenyl-4H-[1,2,4]triazol-3-yl)-pyridine (*ptpy*) derivatives as coordinating ligands through a number of experimental and theoretical approaches. The presence of the fluorine and trifluoromethyl substituents is found to affect both the emission energy and the localization of the lowest excited triplet states, which are characterized as local excitations of the chromophoric ligands (*ppy* or *ptpy*) by DFT calculations. The admixture between metal-to-ligand charge-transfer (MLCT) and ligand-to-ligand charge-transfer (LLCT) is small and their contributions are strongly dependent on the energy gaps between the relevant molecular orbitals.

The sky-blue emitting phosphorescent compound Ir(4,6-dFppy)$_2$(acac) has been doped into matrices and studied under ambient conditions as well as at low temperatures by Rausch et al. (2009). The emitting triplet state is found to be of MLCT character, and the polycrystalline and amorphous hosts are found to show distinct influence on the emissive properties. A clear difference is found through comparison with the similar Ir(4,6-dFppy)$_2$(pic) complex, which could be explained by the different effects of acac and pic ligands on the iridium d-orbitals, leading to different zero-field splittings, radiative emission rates and phosphorescence quantum yields. Highly resolved spectra reveal the importance of the spin-orbit coupling effect related to the emission from individual triplet sub-states. The authors emphasized that the complex symmetry and matrix effects are important factors that affect the performance of OLED devices.

Byun et al. (2007) have synthesized a number of bis-cyclometalated iridium(III) complexes with a common ancillary ligand ZN (3,5-dimethylpyrazole-N-carboxamide), which emit in the sky blue region. DFT calculations show that the cyclometalating ligands contribute negligibly to the HOMO while the ZN ligand is the main contributor together with the iridium d-orbitals. Moreover, it is found that the Ir(MeOF$_2$ppy)$_2$ZN complex possesses the largest phosphorescence quantum efficiency and the lowest nonradiative emission rate. The solution-synthesized organic light emitting device (OLED) of Ir(F$_2$ppy)$_2$ZN doped in a blend of polystyrene and m-bis(N-carbazolylbenzene) has shown an efficiency of 7.8 cd A^{-1} (Byun et al. 2007).

Takizawa et al. (2007) have prepared and systematically studied a series of new blue-phosphorescent iridium(III) complexes containing 2-phenylimidazo[1,2-a]pyridine (pip) derivatives as ligands. Electron-withdrawing substituents on the pip ligands are found to lower the HOMO energy level and lead to blue-shifted emission wavelengths. Based on

experimental data it is found that the HOMO of the iridium complex with pip ligands is mixed Ir-d, phenyl-π and pip-π in character. The pip ligand is able to shift the emission wavelengths into the blue region and the polymer light-emitting devices (PLEDs) suggest that the pip-based iridium complexes are good phosphorescent materials for OLED applications.
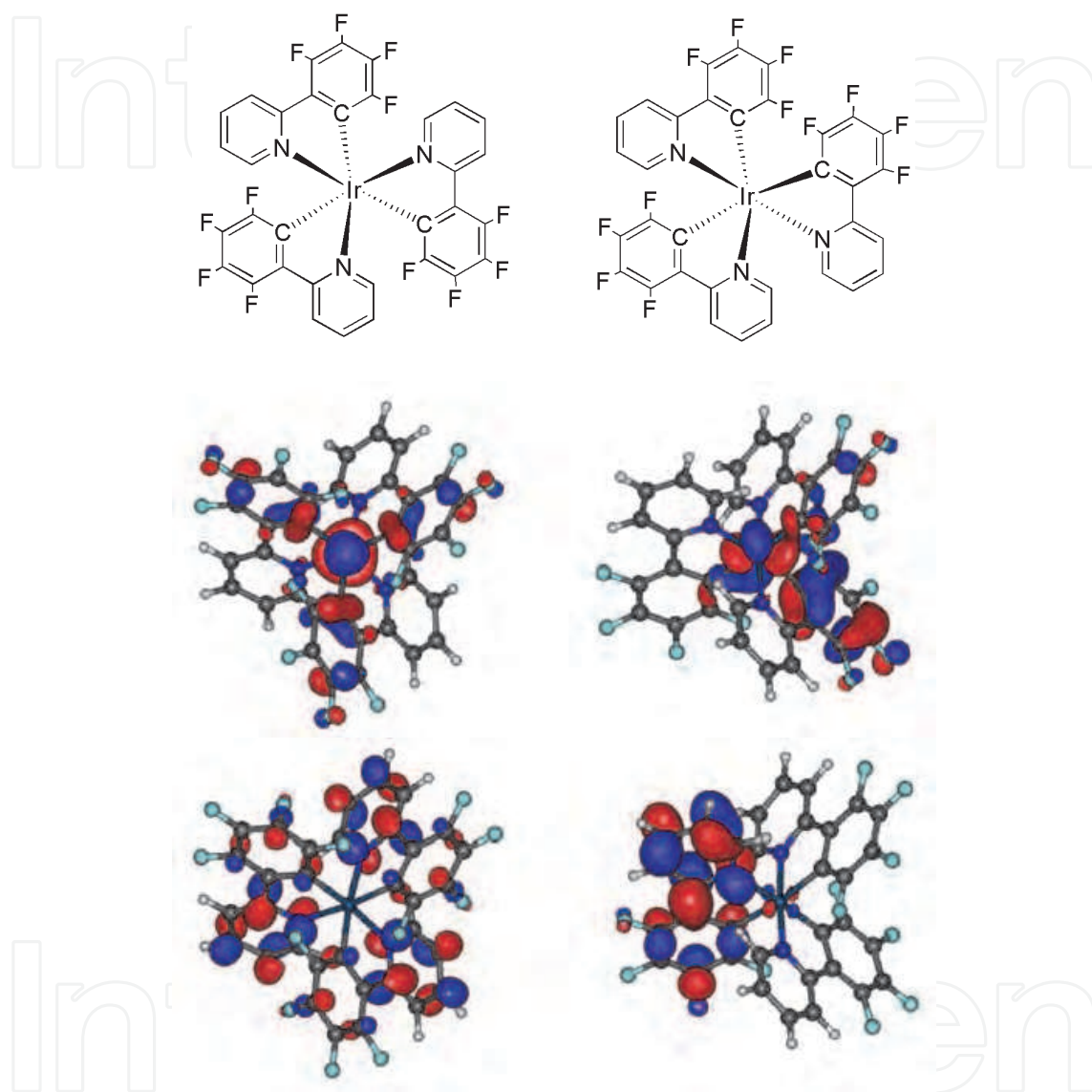

Fig. 3. Structures (top), HOMOs (middle) and LUMOs (bottom) of *fac-Ir(F4ppy)3* (left) and *mer*-Ir(F4ppy)3 (right).

3.4 Introduction of novel ligands

The introduction of novel ligands other than conventional ppy ligands provides the possibility of fine-tuning the spectra of the iridium complexes. For instance, imidazole-based ligands could lead to more delocalized frontier molecular orbitals. Baranoff et al. (2011) have studied two series of heteroleptic bis-cyclometalated Ir(III) complexes with phenyl-imidazole-based ligands, with phosphorescence emission ranging from greenish-blue to orange. The systematic study on these complexes shows that the photophysical and

electrochemical properties could be tuned by changing the substitution pattern on the ligands. DFT calculations suggest that the highest occupied molecular orbital (HOMO) and the lowest unoccupied molecular orbital (LUMO) are more delocalized in complexes with phenyl-imidazole as ligands. Interestingly, the presence of chlorine substitution leads to an unexpected red shift in the emission energy, which could be explained by significant geometrical and electronic relaxation as confirmed by theoretical calculations.

Chang et al. (2007) reported the preparation of a series of new heteroleptic Ir(III) complexes chelated by two cyclometalated 1-(2,4-difluorophenyl)pyrazole ligands (*dfpz*)H and a third ancillary bidentate ligand (L^X). The cyclometalated *dfpz* ligands give rise to a larger π-π* gap in the iridium complexes, and the lowest one-electron excitation are expected to accommodate the π* orbital of the ancillary L^X ligands, which could be modified to fine-tune the phosphorescent emission. The reduction and oxidation reactions are found to occur mainly at the ancillary L^X ligands and the iridium metal site, respectively. The authors have shown a simple and straightforward approach to tune the color by varying the ancillary ligands only (Chang et al. 2007).

Volpi et al. (2009) have studied the cationic heteroleptic cyclometalated iridium complexes with 1-pyridylimidazo[1,5-alpha]pyridine (pip) ligands in order to provide exploitation of an efficient intersystem crossing in OLEDs. Blue luminescence is observed upon excitation of [Ir(ppy)2(pip)]+ with lifetimes between 0.6 and 1.3 μs. TD DFT calculations with solvent effect taken into account reveal that the iridium center contributes significantly to most transitions. Furthermore, a photochemical reaction has been observed to give rise to a new class of cyclometalated iridium complexes with dipyridylketone and deprotonated amide as ligands.

Chou et al. have presented general concepts that have guided important developments in the recent research progress of room-temperature phosphorescent dyes. The authors elaborate on both the theoretical background for emissive metal complexes and the strategic design of the 2-pyridylazolate ligands, aiming to fine-tune the chemical and photophysical properties. The 2-pyridylazolate ligands are incorporated to give rise to the highly emissive transition-metal complexes, which show potential usefulness in the application as OLED dyes. Based on this family of metal complexes, the possibility of tuning the emission toward the near-IR region with for future applications in solar cell and near-IR imaging has been proposed.

Yang et al. (2008) studied neutral mixed-ligand Ir(N=C=N)(N=C)X complexes which are not emissive at room temperature but exhibit strong phosphorescence at 77 K. The 0-0 transition energies are located at around 450 nm with lifetimes of 3-14 μs. Through temperature-dependent lifetime measurements and unrestricted density functional theory calculations, the mechanism and pathway of thermal deactivation are analyzed in detail. The calculated activation energies of approximately 1800 cm^{-1} are in excellent agreement with the observed values.

Liu et al. (2007a) have presented calculations on geometries, electronic structures, and spectroscopic properties of a series of cationic iridium(III) complexes with C^N and PH$_3$ ligands. The geometries at the ground state and the excited state are optimized at the B3LYP/LANL2DZ and CIS levels of theory, respectively. The HOMOs are found to localize on the iridium atom and the C^N ligands, while the LUMOs are dominantly localized on the C^N ligand. TD DFT calculations with solvent effects taken into account by the polarized continuum model provide absorption and phosphorescence wavelengths in acetonitrile solution, and the low-lying absorptions are assigned as the d$_{yz}$(Ir) + π(C^N)] →

π*(C^N) transition. The computations also suggest that the phosphorescent emission wavelengths could be blue-shifted by introducing π electron-withdrawing groups and by suppressing the π-conjugation in the C^N ligand.

Liu et al. (2008) also investigated the photophysical properties of heteroleptic iridium complexes containing carbazole-functionalized β-diketonates. The authors have studied the influence of the triplet energy level of the ancillary carbazole-containing ligand on the photophysical and electrochemical behavior, and found that the superposition of the state density map of the triplet energy levels between the β-diketonate and the Ir(C^N)$_2$ fragment is the key factor to obtain strong ^{3}LC or ^{3}MLCT-based phosphorescence and high photophysical performance. DFT calculations reveal that the lowest excited state is mainly determined by the C^N ligand but not by β-diketonate when there is large difference between the triplet energy levels of the two parts, providing satisfactory explanation for experimental results.

The photophysical properties of facial and meridional tris-cyclometalated iridium(III) complexes containing 2-phenylpyridine and 1-phenylisoquinoline ligands have been reported by Deaton et al. (2010). The facial isomers show similar photophysical properties in 2-MeTHF solutions, indicating that the emission occurs based on the *piq* ligand(s). By comparing the photophysical properties between *fac*-Ir(*piq*)$_3$ and fac-Ir(*piq*)(*ppy*)$_2$ the effect of the *piq* ligand is revealed; it is found that the quantum yield is higher in *fac*-Ir(*piq*)$_3$ than that in *fac*-Ir(*piq*)(*ppy*)$_2$, suggesting a larger nonradiative rate in the latter compound. The meridional complexes have much lower quantum yields in solution comparing with their facial counterparts, and the difference between *mer*-Ir(*piq*)(*ppy*)$_2$ and *fac*-Ir(*piq*)(*ppy*)$_2$ is interpreted by more π-π* character and less MLCT character in the former compound. The authors have shown that the phosphorescent decay is very efficient and may be used in OLEDs.

3.5 External modulation of Ir(III) phosphorescence

Considering the development of molecular switches that respond to external electric or photonic stimuli, it is interesting to introduce such a switching unit into the iridium complexes to realize a controllable phosphorescent emission. Zapata et al. (2009) have studied a heterobimetallic Ir(III) complex with a ferrocenyl azaheterocycle as ancillary ligand, which acts as a redox-fluorescent molecular switch. The ancillary ligand consists of a redox-acitve ferrocene unit and a 1,10-phenanthroline chelator coordinating with the iridium center. By tuning the oxidation state of the ferrocene through electrochemical stimuli, the emission intensity of the iridium complex can be modulated. This is an interesting example of the effective control of emission in iridium compounds. Besides, Tan et al. (2009) reported the photochromic iridium(III) complex (Py-BTE)$_2$Ir(acac) in containing two bis-thienylethene (BTE) switching units and one iridium(III) center. This molecule has shown distinct photo-reactivity and photo-controllable phosphorescence due to the combination of the photochromic BTE switch and the highly luminescent iridium(III) complex into one molecule. Through photo-induced isomerization, the phosphorescence is almost completely quenched by the closed-ring form of the BTE unit. Through DFT calculations, Li et al. (2010) have shown a monotonic relationship between the metal character of phosphorescence and the radiative deactivation rate constant function and rationalized the non-radiative deactivation rate using the energy gap law, leading to a theoretical interpretation of photochromic modulation of the iridium(III) phosphorescence.

4. Other new OLED materials

In the following we will consider our own experimental design of new materials for molecular electronics, electroluminescent and solar energy conversion devices. First we consider improvements of light-emitting and ETL materials, which do not include transition-metal complexes.

4.1 Modification of hole transport and electron transport layers

In Ref. (Xie et al, 2005) a new soluble 5-carbazolium-8-hydroxyquinoline Al(III) complex was synthesized and used in OLEDs as a dipolar luminescent material instead of Alq_3 (Scheme 1), which was the milestone emitting ETL material during two decades. An excellent capacity of electron transportation of Alq3 is determined by effective LUMO overlap between neighboring molecules (A_4 and A_3 in Fig. 1b). But the overlap of HOMOs, which governs the hole-transport (overlap between HOMO of molecules A_2 and A_1 in Fig. 1b) is very low. That is why we need to use an extra HTL material like NPB in order to obtain an effective OLED function. Carbazole derivatives are also widely used as hole-transport materials between the emitting layer and the anode. The idea to combine ETL and HTL properties and unite carbazole and Alq_3 moieties in a new luminescent material has been realized (Xie et al, 2005). The new soluble synthesized complex includes carbazolium substituted in a *para*-position to the oxygen in Alq_3. The highest spin density is at the HOMO of the ionized hole at this C-5 carbon atom position in the Alq_3 quinolate moiety. The electron-donating carbazolium substituent in the C-5 position causes a red-shift in the emission and absorption spectra of a new aluminum complex. The photoluminescence spectrum indicates an effective intramolecular singlet energy transfer from the carbazole groups to Alq_3 (no carbazole emission). The half oxidation potential of the new complex provides the HOMO energy (-5.51 eV) which is higher than that of Alq_3 (-5.9 eV). This significant improvement of the hole transport property is determined by the fact that the HOMO is mostly localized on the carbazole groups (Xie et al, 2005). The new complex being soluble is much better than Alq3, which must be vacuum deposited in fabrication of OLEDs. The main interest in soluble luminescent materials with high ETL and HTL properties lies in the scope for low-cost manufacturing, like spin coating, which is in line with the current trend to fabricate OLEDs from solutions.

4.2 Functionalization of nonmetallic photoluminescent complexes for red-emititng OLEDs

For full color displays red-emitting materials are required (besides green and blue emitters discussed above). Materials with red emission are usually achieved by doping red dyes (e.g., porphyrins) into a host matrix with a large band gap (Li et al. 2007). Because typical organic red dyes are large π-conjugated planar systems, they are prone to aggregate and quench their luminescence. Such organic dyes being highly emissive in dilute solutions become non-luminescent in the solid state. Many functional groups like oligo-fluorenes, truxene, indoles, which act as light-harvesting antenna and prevent aggregation, have been attached to porphyrins to obtain novel red-emitting materials for OLEDs. Bisindolylmaleimides provide wide luminescence bands in the range 550-650 nm and have also been found useful in fabrication of white color OLEDs (Ning et al. 2007a). In Ref. (Li et al. 2007) the bisindolylmaleimide (BIM) group, conjugated with tetraphenylporphin (TPP) in the form of dyad (PM-1) and pentamer (PM-2), have been sensitized and found to serve as good

candidates of red-light emitting materials for OLEDs. These dendrimers have been prepared through imidization of bisindolylmaleic anhydride with aminoporphyrins. The long hexyl chains on the BIM groups improve solubility and suppress the aggregation in the solid state (Li et al. 2007). The new sensitized porphyrin dendrimers, PM-1 and PM-2, exhibit an intense Soret band (420 nm) and week Q-bands (500-650 nm) in the absorption spectra in dilute THF, which are typical for the TPP itself. The Soret band is slightly red shifted and broadened (compared with TPP) and new UV absorption occurs at 290 nm. The latter coincides with the BIM band and increases when the numbers of BIM groups increase in the dendrimers. Week additional BIM absorption occurs at 480 nm, which corresponds to charge transfer from the indolyl to the maleimide moiety. The luminescence spectra of all dendrimers exhibit characteristic emission of porphyrin, which consists of two vibronic Q_x bands: the strong 0-0 and week 0-1 peaks at 660 and 750 nm, respectively (Minaev et al. 2005). The dendrimer emission is much more intense than that of TPP, especially for the 0-0 band. This indicates an efficient singlet energy transfer from the BIM-antenna groups to the porphyrin ring. The through-bond energy transfer by the Förster intramolecular mechanism provides efficient fluorescence of the porphyrin moiety with the quantum yield in PM-2 being twice as large in comparison with TPP. The porphyrin dendrimer PM-2 with four BIM groups exhibits much stronger emission comparing to the PM-1 dye with only one BIM group due to enhanced antennae harvesting effects.

OLEDs made with solid film PM-2 spin-coated on quartz plate (ITO/PEDOT/PVK/PFO +PBD: PM-2 (5%)/Ba/Al) show pure red emission. The external quantum efficiency (0.13%) demonstrates effective EHP recombination and energy transfer in this EML. Another OLED device with 2.5% PM-2 doped within the PFO+PBD emissive layer exhibits higher external quantum efficiency (0.2%) and luminance maximum (101 cd m^2), but the chromaticity is not so pure (Li et al. 2007).

BIM derivatives themselves have also been used as non-doped red light-emitting materials (Ning et al. 2007a). Their solid state fluorescence quantum yield can be dramatically changed by introduction of different substituents on the non-conjugated linkage to the BIM skeleton. The OLED configuration (ITO/NPB/maleimide/TPBI/LiF:Al) with BIM derivative (1S) of 2,3-bis(N-benzyl-2'methyl-3'-indolyl)-N-methylmaleimide reaches the brightness 393 cd m-2 at 100 mA cm-2. Though the performance of such non-doped red organic light-emitting materials is not as good as the conventional doped ones, they are more promising for mass production (Ning et al. 2007a). OLEDs based on non-doped host EML can simplify the manufacturing significantly.

As indicated earlier, iridium(III) complexes are promising materials for applications in OLEDs, due to their strong spin-orbit coupling, intense phosphorescence, high quantum efficiency and tunable emission wavelengths. In most iridium complexes the HOMOs are found to locate on the metal center and on π-orbital of the ligands, and the LUMOs are delocalized on the π*-orbital of the ligands. Electron-hole recombination in the doped emitting layer results in a mixed MLCT and ILCT triplet state, leading to efficient phosphorescence. By utilizing the triplet emission energy in OLED devices, iridium complexes are able to significantly enhance the efficiency of electroluminescence. However, cheaper organic molecules and supramolecular aggregates which utilize only singlet excited states for charge carrier recombination and energy transfer are still useful for low-cost OLED applications and for solar energy conversion. The position of HOMO and LUMO of the dye and their redox electrochemical parameters with respect to the electrode materials are crucial not only in OLEDs but also for photovoltaic devices. We shall in the coming

section consider two promising types of such devices; dye-sensitized solar cells (DSSC) and organic semiconductor devices with triplet excitons.

5. Metal complexes for dye-sensitized solar cells

In order to see some common features in light emitters (OLED) and absorbers (DSSC) let us consider first a typical solar cell. DSSCs of the Grätzel type mainly consist of an optically transparent photoanode (lower Fluorine-doped tin oxide (FTO) glass sintered with TiO_2 nanocrystals), dyes adsorbed on mesoporous nanocrystalline TiO_2, electrolyte, and a cathode which consists of a platinum thin film layer sputtered on the upper FTO layer (Fig.4).

Fig. 5 shows the main carrier transport channels. At first, the incident light (hv) is absorbed by the sensitizer dye, the electrons of which are excited from the HOMO to the LUMO. Consecutively, the photogenerated electrons are injected from the LUMO of the dye to the conduction band (CB) of the TiO_2 (channel (a) in Fig. 5). The oxidized dye will later be reduced by the redox couple, channel (b), that recieves electrons from the counter electrode (cathode). Apart from these normal electron transfer channels, there are some other undesirable carrier transport channels, such as charge recombination of electrons from TiO_2-CB to the dye cations (c) and to the redox couples (d), and excited dye quenching by direct decay from LUMO to HOMO (e).
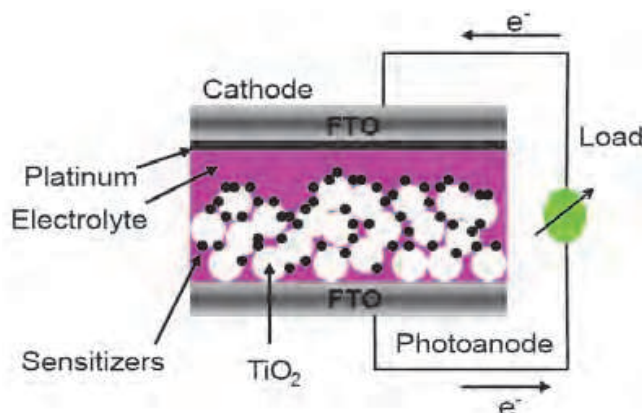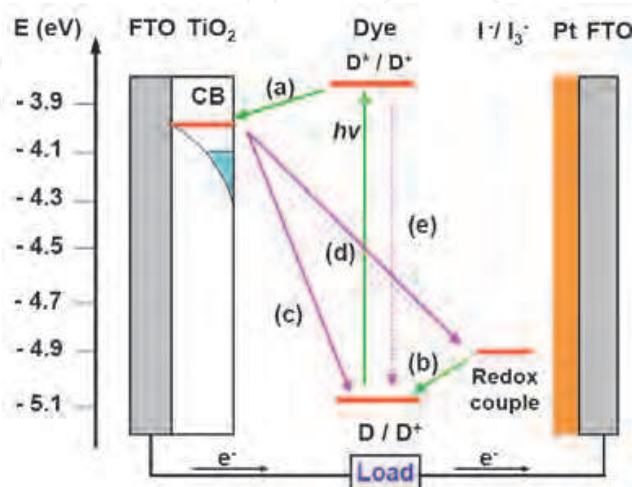

Fig. 4. Schematic structure diagram of DSSCs.

Fig. 5. Energy band structure and major electron transfer processes in DSCs.

Among all the constituent components in DSSCs (Fig. 4), the sensitizer, being charged with the task of the light absorption and electron injection, is generally regarded as the most crucial one for the overall efficiency. Since the first report by Grätzel and coworkers, the metal complex dyes are generally considered as the best sensitizers for DSSCs (O'Regan et al. 1991). During the development of DSSCs, a benchmark is given by the introduction of dye N3 (*cis*-dithiocyanato bis(2,2'-bipyridine-4,4'-dicarboxylate)ruthenium-(II)), which achieves efficiency over 10 % (Nazeeruddin et al. 1993. The other famous dye N719 is similar to N3, differing by the number of protons). A great deal of efforts were made to optimize the performance of metal complex dyes by molecular modification, meanwhile, the relationship between the sensitizer structure and performance has been extensively studied. In this section, we mainly focus on the development of metal complex sensitizers, which are similar to chromophores developed for OLEDs.

5.1 Extension of the absorption spectra

Although the efficiency of N3 is as high as 10 %, its absorption spectrum is mainly located in the visible region, and is quite weak in the near-infrared region of the Sun radiation. To improve the efficiency of DSSCs based on Ru complexes further, the absorption spectrum must be extended (Ning et al. 2009). For this purpose a number of new dyes have been sensitized.

5.1.1 Introduction of additional substitute on one of the bipyridine ligand in N3

The group of Wu and the Wang's group have reported a new kind of ruthenium complexes such as C101 (Scheme 2) (Gao et al. 2008), with high molar extinction coefficients by the addition of alkyl-substituted thiophene on the spectator ligands, with a motivation to enhance the optical absorptivity of the sensitizer. Along with the acetonitrile-based electrolyte, the C101 sensitizer achieved a strikingly high efficiency of 11.0-11.3%. The cells based on a low-volatility 3-methoxypropionitrile electrolyte and a solvent-free ionic liquid electrolyte, show conversion efficiency over 9.0%. In addition, this DSSC is highly stable under full sunlight soaking at 60°C during 42 days. It was speculated that alkyl chains (C_6H_{13}) can create a hydrophobic environment to improve the stability of the cells. Another possible reason might be that alky chains facilitate formation of a more compact sensitizer layer to prevent the approach of the electrolyte to the TiO_2 surface. Substitution of sulfur by selen in the dye C101 produces an effective sensitizer (C105) (Gao et al. 2009). TD DFT calculations of these dyes (Baryshnikov et al. 2010) indicate much more intense absorption of C105 with respect to the N3 dye and explain the negative solvatochromic effect, which is a sequence of the selenophene conjugation with the bpy ligand. Strong changes of the Ru-N and C-C bond lengths in the substituted bpy ligand also indicate the π-conjugation effect with selenophene. Besides, it supports the planar structure of the ligands (Baryshnikov et al. 2010). An intense absorption band of C105 at 746 nm is determined by two transitions: from HOMO to LUMO+2 with small admixtures of other excitations and from HOMO to LUMO+3. The highest occupied MOs in the C101 and C105 dyes are localized on the 3d orbitals of the Ru ion and on the N=C=S groups. Four quasi-degenerate vacant MOs in C105 are localized on the bpy ligands with some admixture from the metal. Thus the sun light induces the MLCT and NCS→bpy charge-transfer transitions. All types of bpy ligands are involved, something that provides an efficient electron injection through the carboxyl-groups.

Wu et.al have introduced ethylene-dioxythiophene groups on the bipyridine ligand, which further extended the absorption spectra compared with the thiophene ligand (Chen et al. 2007). The sensitizer SJW-E1 (Scheme 2) shows higher efficiency than N3 under the same conditions due to the extension of the electron donor ligand, which can uplift the HOMO energy edge and reduce the energy waste between the HOMO energy of the sensitizer and the redox couple. Based on the thiophen-substituted complex, Wu et. al further developed a new ruthenium-based dye (CYC-B6S, Scheme 2) in which alkyl-substituted carbazole moieties were incorporated in the thiophene-substituted bipyridine ligand (Chen et al. 2008). Compared with the N3 dye, the unique ancillary ligand in CYC-B6S is well-designed to enhance the light-harvesting capacity with the thiophene unit to further enrich the spectral response. Wang et.al developed a new Ru complex sensitizer K19 (Scheme 2) with a styryl unit attached to the bipyridly ligand (Kuang et al. 2006). The addition of this styryl ligand significantly enhanced the light absorbing capability. In addition, the DSS cells based on the K19 sensitizer also show an excellent photochemical stability. After 1000 h of light soaking at 60 °C, no drop in efficiency was observed for the cells covered with an ultraviolet absorbing polymer film.
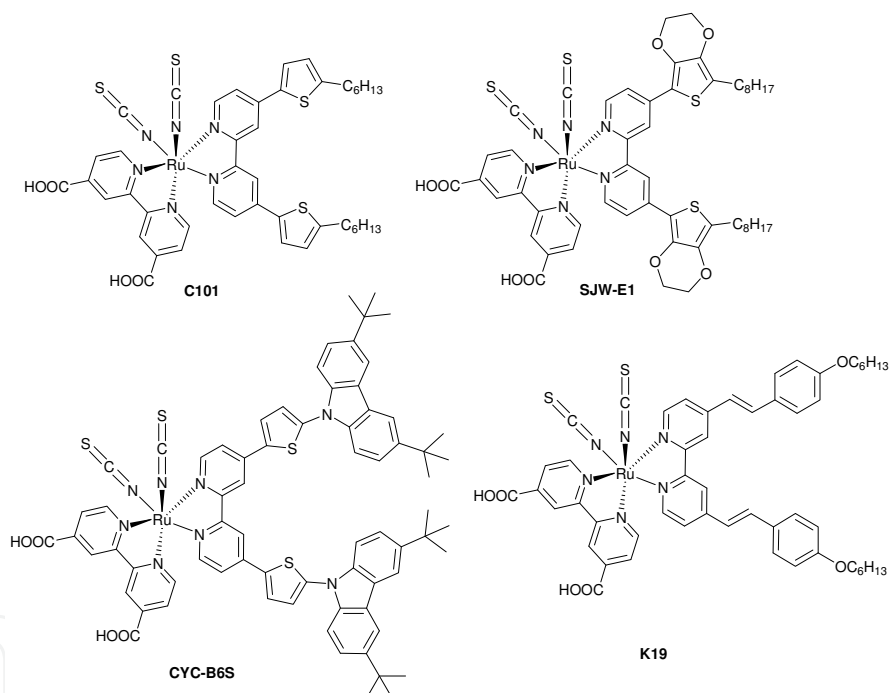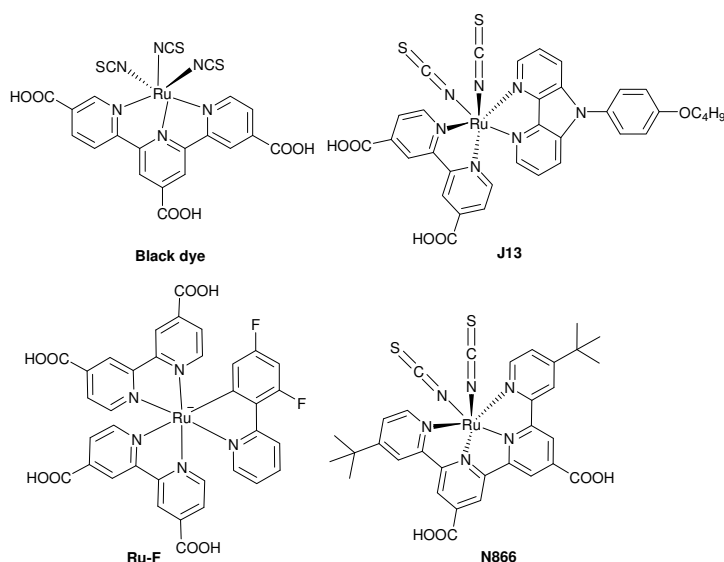

Scheme 2.

5.1.2 Modification of the ligand

A series of panchromatic ruthenium(II) sensitizers (black dye, Scheme 3) derived from carboxylated terpyridyl complexes of tris-thiocyanato Ru(II) has been developed by Grätzel's team (Nazeeruddin et al. 2001). Due to the presence of three thiocyanate ligands, the absorption spectrum is obviously red-shifted compared with complexes which have two thiocyanate ligands. The black dye, when anchored to nanocrystalline TiO$_2$ films, achieves very efficient sensitization over the whole visible range extending into the near-IR region up to 920 nm, yielding over 80% incident photon-to-current efficiencies (IPCE). Employing this dye the highest record conversion efficiency up to now, 11%, was achieved.

Jin et.al synthesized a novel kind of Ru complex sensitizer with a triarylamine-ligand (Jin et al. 2009). Under standard global AM 1.5 solar conditions, the J13 (Scheme 3)-sensitized solar cells demonstrate short circuit photocurrent densities of 15.6 mA/cm², open circuit voltages of 700 mV, fill factors of 0.71, and overall conversion efficiencies of 7.8%, which is comparable to the N719 dye under which identical measurement conditions gives 7.91%. DFT/TDDFT calculations indicate that the triarylamine ligand acts as an electron donor in a manner similar to the thiocyanato ligands and Ru metal. However, no obvious bathochromic shift of the absorption spectrum was observed.

Grätzel and coworkers developed a novel thiocyanate-free cyclometalleted ruthenium sensitizer (Ru-F, Scheme 3) with electron acceptor fluorine atoms substituted on one ligand (Bessho et al. 2009). Density functional theory (DFT) and time-dependent DFT (TDDFT) calculations show that the HOMO is located mostly on ruthenium and the cyclometalated ligands. Molecular orbital analysis confirms the experimental assignment of the redox potentials, and TDDFT calculations allow an assignment of the visible absorption bands. The DSSC based on Ru-F exhibits a remarkable IPSE value of 83%.

Black dye   **J13**

**Ru-F**   **N866**

Scheme 3.

A ruthenium complex N886 (Scheme 3) with quarterpyridine as a ligand has been developed by Grätzel's group (Barolo et al. 2006). The absorption spectrum of the N886 complex shows metal-to-ligand charge-transfer transitions in the entire visible region. The TD DFT method qualitatively reproduces the experimental absorption spectra. The absorption bands were assigned to the mixed Ru/SCN-to-quaterpyridine charge-transfer transitions, which extend from the near-IR to the UV regions. Dramatic red shift of the absorption spectrum compared with N3 is observed. A DSSC the based on panchromatic sensitizer N886 complex shows an overall conversion efficiency of 5.85%.

5.2 Molecular modification of the Ru complex in order to reduce charge recombination

The charge recombination between the injected electrons in TiO2 and oxidized sensitizer or redox couple can significantly decrease the conversion efficiency of the DSSCs (Ning et al. 2010). Much efforts have been devoted to reduce these processes.

5.2.1 The task to reduce charge recombination between the oxidized sensitizer and TiO$_2$

In recent years, it was reported that the introduction of a triarylamine unit can increase the distance between the TiO$_2$ surface and the sensitizer electron-donor unit where the charge recombination normally occurs, and thus to reduce the charge recombination between sensitizer and TiO$_2$. Durrant et al. developed the sensitizer Ru-1 (Scheme 4) with a triphenylamine unit connected to the Ru complex, which showed higher efficiency than the sensitizer without the triphenylamine (Hirata et al. 2004). The observed suppression of the carriers recombination is attributed to an increase in the physical separation between the dye cation and the metal oxide surface. Bonhôte and coworkers have studied the charge recombination process in a series of Ru dyes connected with triphenylamine (Bonhôte et al. 1999). The lifetime of injected electrons in TiO$_2$ is enhanced by a significant factor of 100 times after the incorporation of those units in their model system (without I$^-$/I$_3^-$ redox couples so that the carrier recombination mostly occurs between the oxidized dye and the injected electrons). In the model system, the sensitized nanocrystalline TiO$_2$ film employing the Ru-4 dye (Scheme 4) achieves a remarkably long lifetime of 4 s for injected electrons in TiO$_2$.
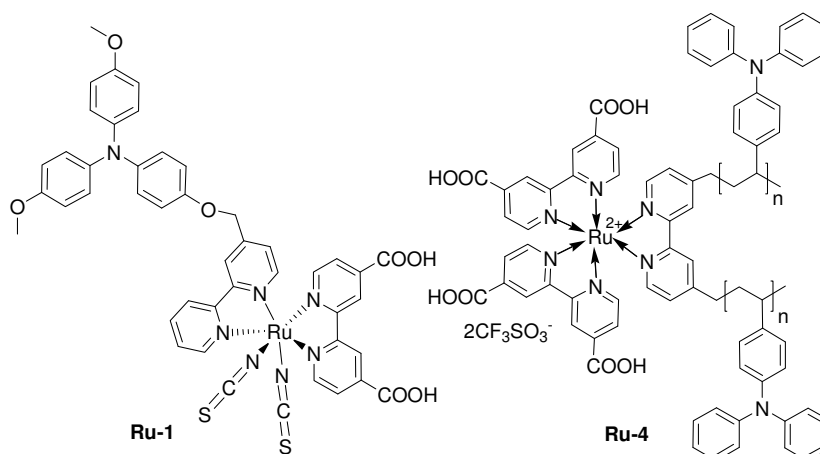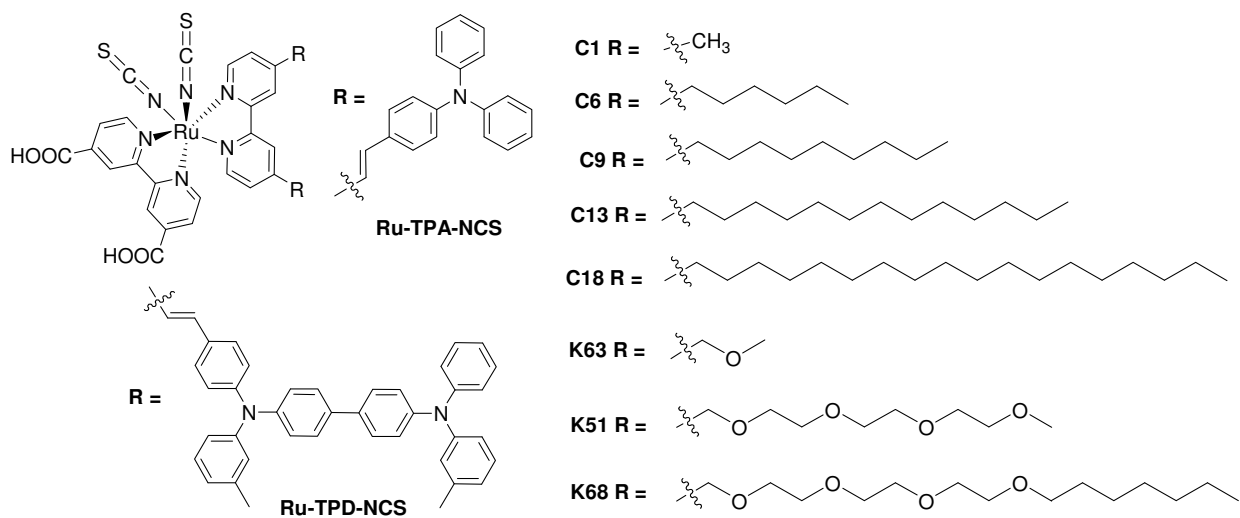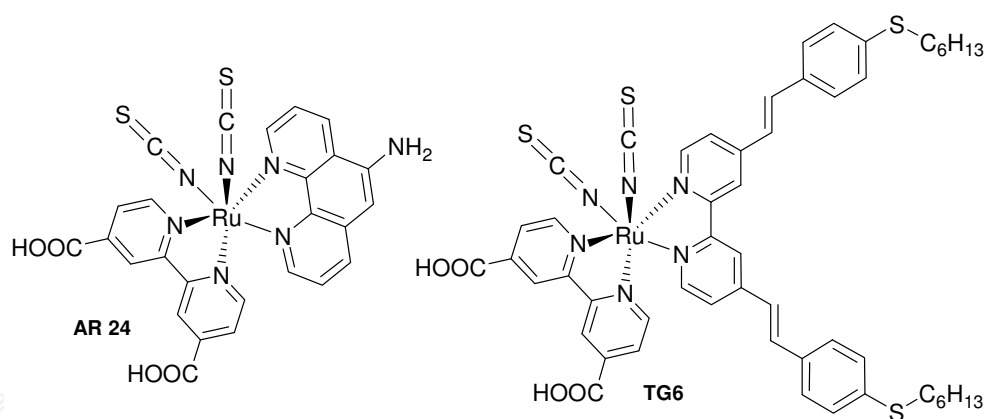

Scheme 4.

5.2.2 The task to reduce the charge recombination between oxidized sensitizer and redox couple

Except the charge recombination between TiO$_2$ and the oxidized sensitizer, the electron transfer from TiO$_2$ to the electrolyte will decrease the efficiency as well. It was reported that the starburst structure is also suitable for Ru dyes to reduce the charge recombination between TiO$_2$ and electrolyte. Haque and coworkers reported significantly reduced charge recombination between TiO$_2$ and redox couple by the connection of triphenylamine on the ligand (Haque 2005). Thelakkat and coworkers developed Ru dyes (Ru-TPD-NCS, Ru-TPA-NCS) with triarylamine substituents and applied them in solid state dye-sensitized solar cells (SDSCs) (Scheme 5) (Karthikeyan et al. 2007). The exterior starburst triarylamine can effectively reduce the carrier recombination between the injected electrons and redox couples, leading to higher V$_{oc}$ and efficiency than N719. Kroeze and coworkers found that for Ru-complex-sensitizer-based DSCs, charge recombination can be reduced by connecting

long alkyl chains (Fig. 4) (Schmidt-Mende et al. 2005). Snaith and coworkers obtained a much prolonged carrier lifetime by linking oxyethylene and/or diblock ethylene-oxide:alkane pendent groups to the Ru sensitizers (Snaith et al. 2007). By suppressing the carrier recombination, V_{oc} of SDSCs based on K68 reach as high as 0.93 V, and the total energy efficiency is 5.1% under AM 1.5 irradiation.

Scheme 5.

Scheme 6.
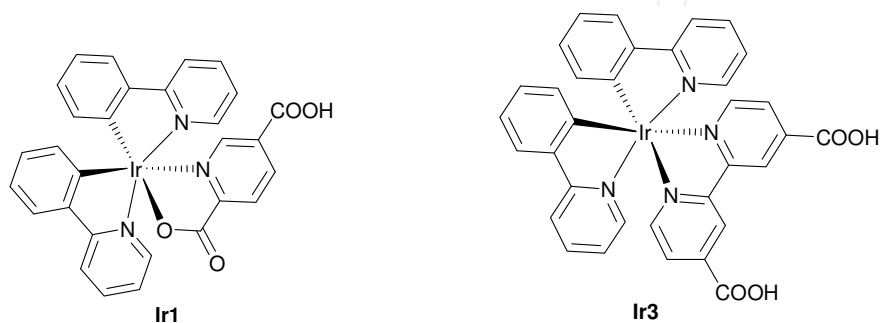
Scheme 7.

In addition to the blocking effect of the sensitizer, O'Reagan and coworkers recently found another potential factor that is crucial to determine the charge recombination, namely that the dye molecules can form complexes with the redox couple, and thus enhance the recombination reaction between electrons in TiO₂ and the electrolyte (O'Regan et al. 2009). They observed that the presence of an amine AR24 (Scheme 6) group in the sensitizer can significantly aggravate the charge recombination because of its strong iodide binding capability (Reynal et al. 2008). In addition, they found that the charge recombination of the sensitizer with an lkoxy group (K19) was clearly more serious than for the alky sulfide substitute (TG6) (O'Regan et al. 2009a). The difference was attributed to the different complexation capability with iodide of the sensitizer. However, up to now, the detailed mechanism of the complex is not clear.

5.3 The task to increase the electron injection efficiency

To increase the electron injection efficiency of DSSCs, it is critical to decrease the distance between the sensitizer acceptor and the TiO₂. An effective strategy might be the adoption of multi-anchor units. Tian et al. investigated a series of iridium sensitizers with one or two carboxyl anchor groups. It was found that the efficiency of a sensitizer with two carboxyl units (Ir3, Scheme 7) is pronouncedly higher than for a sensitizer with a single carboxyl unit (Ir1, Scheme 7) (Ning et al. 2009a).

Another factor that affects the electron injection efficiency is the non-radiative decay of the sensitizer, which results in energy loss. Tian et. al investigated the relationship between the emission quantum yield and the electron injection efficiency of sensitizers (Ning et al. 2009a). It was found that the electron injection efficiency is consistent with the luminescence quantum yield of the sensitizer. Since less non-radiative decay guarantees high luminescence quantum yield to enhance the electron injection efficiency, it is important to reduce the non-radiative decay which arises mainly from the molecular vibrations. The ethylene linkage is susceptible to isomerization upon irradiation, which leads to vibrational energy loss. For sensitizers with several ethylene units, the efficiencies are generally low (Ning et al. 2009).

The Ir1 complex (Scheme 7) synthesized recently for DSSC devices (Ning et al. 2009a) is very similar to Ir(ppy)₂(pic) species (Scheme 1), used for OLEDs (Nazeeruddin et al. 2009, Minaev et al. 2009). The only difference is the presence of the COOH group in the 2-pyridinecarboxylate (picolinate) moiety, which is necessary for adsorption on the TiO₂ surface in DSSCs. The LUMO in both complexes is localized entirely on the picolinate ligand; in the Ir1 species the LUMO has a large contribution from the carboxyl group (Ning et al. 2009a). This is important for the LUMO overlap with the surface of the semiconductor and for the electron injection efficiency of the DSSC. The photocurrent action spectrum of the TiO₂ electrode sensitized by Ir1 dye indicates that the weak absorption at 490 nm (first HOMO→LUMO transition) produces electron injection, which is increased up to 80% IPCE at 440 nm ($S_0 \rightarrow S_2$ absorption). The S_2 state has no admixture of the carboxyl group, which means that injection occurs after the fast $S_2 \rightarrow S_1$ relaxation.

Introduction of the N,N-dimethylamino group into the *para*-position of the picolinate ligand provides a quite efficient CIC dopant (N984) for the emissive layer in OLEDs (Nazeeruddin et al. 2009). This is explained by SOC calculations and the large change in the T_1 state wave function (Minaev et al. 2009) of the Ir(ppy)₂(pic) complex. In the absence of the dimethylamino group the antibonding π MO of picolinate ligand shifts down and becomes

the LUMO which gets lower by 0.38 eV in comparison with the N984 complex. This is in agreement with the cyclic voltammogram of the N984 complex, which shows a reversible couple at 0.61 V versus ferrocene Cp_2Fe/Cp_2Fe^+ redox couple due to the Ir(III/IV) reduction-oxidation cycle. Such a reduction potential of N984 demonstrates that the LUMO is located on the 2-phenylpyridine ligand rather than on the aminopicolinate ancillary ligand, the lowest unoccupied MO of which is destabilized by the presence of the N,N-dimethylamino group. The changes of MO energy levels determine the differences in UV-vis absorption and phosphorescence spectra induced by the insertion of the N,N-dymethylamino group in the 4-position of the picolinate ancillary ligand (Minaev et al. 2009). One can thus see that common quantum-chemical studies of the similar chromophores used in OLED and DSSC devices (Minaev et al. 2009, Ning et al. 2009a) can help to understand the most essential electronic structure features responsible for emissive and electron injection properties of cyclometalated iridium complexes.

6. Organic solar cells based on a bulk heterojunction architecture

Organic solar cells (OSC) based on a bulk heterojunction architectures can be realized by mixing of two solutions of organic semiconductors with different electronegativities and subsequently spinning a film (Köhler & Bässler 2009). The photoexcited state in one material diffuses to the interface of the other where dissociation occurs. The size of the phase separation between the two materials should be on the same length scale as the exciton diffusion length. This also requires a percolation path for separated charges to be sufficient to reach the corresponding electrodes. Fabrication of the film can be optimized by proper annealing, solvent mixture, and by spin-coating a blend. In this way a solar cell based on a bulk heterojunction (fullerene/low-bandgap polymer) has been obtained recently with a PCE of 5.5% (Köhler & Bässler 2009). The triplet excitons have longer diffusion length compared to singlets and this could be used as advantage for such OSCs. Despite the slow Dexter mechanism for the triplet exciton transfer, the large lifetime provides a triplet diffusion length ranging from 20 to 140 nm in amorphous organic films, while for singlet excitons it is typically in the range 10-20 nm (Köhler & Bässler 2009, Köhler at el. 1994).

From the energetic point of view OSCs based on triplet excitons are less favorable than usual polymer solar cells based on singlets (Köhler et al. 1994). Triplet excitons are more tightly bound than singlet excitons (by two exchange integrals, $2K_{ij}$) and this increases the barrier for exciton dissociation. It can be overcome by suitable LUMO energy level matching. Anyway, this leads to waste of a fraction of the absorbed solar energy. The maximum possible PCE is predicted to be about 11% for OSCs based on singlets and is likely to be somewhat lower for triplet solar cells (Köhler & Bässler 2009). In the first produced triplet OSC the material used was a conjugated platinum(II)-containing polymer (Köhler et al. 1994) of the form trans-$[-Pt(PBu_3)_2C\equiv CRC\equiv C-]_n$, where R= phenylene. The efficiency of single-material OSCs based on such Pt-polymers with triplet excitons are comparable to that of analogously built solar cells with singlet excited states (Köhler et al. 1994). When the Pt-polymers with triplet excitons were incorporated in OSCs based on a bulk heterojunction architecture with fullerene the PCE increased up to 0.3% (Köhler et al. 1996). These Pt-polymers have blue absorption (Minaev et al. 2006; Lindgren et al. 2007), while solar light peaks in the red. Thus for practical applications other Pt- and Pd-containing polymers have been synthesized with conjugated spacers R which have strong

electron-acceptor character and various such heterojunction devices have been fabricated using this concept (Köhler & Bässler 2009).

7. Conclusions

In this review we have discussed the understanding and design of optimal organometallic chromophores for light-emitting layers in OLEDs and for light-absorbing dyes and charge separation in DSSC interfaces. As an illustrating example, electro-luminescence OLED devices based on cyclometalated Ir(III) complexes (CICs) are discussed in some detail with special attention to spin-orbit coupling effects and triplet state emission. In pure organic polymers, like PPV or PPP, the energy stored in triplet states cannot be utilized in order to increase the emissive efficiency of OLEDs. With CICs as dopants the electroluminescence is enhanced by harnessing both singlet and triplet excitons after the initial charge recombination. Because the internal phosphorescence quantum efficiency is high - as high as 100% can theoretically be achieved - these heavy metal containing emitters will be superior to their fluorescent counterparts in future OLED applications. That has spurred quantum theory research on internal magnetic perturbations in such heavy transition metal complexes. The spin conservation rule as well as its violation in modern phosphorescent OLEDs is of principal importance in optoelectronics and spintronics applications. Synthesis of new materials for OLEDs can be rationalized if proper understanding of spin quantization and spin-orbit coupling is taken into account. Moreover, since the manufacturing of a full color display requires the use of emitters with all three primary colors, *i.e.* blue, green and red, the rational tuning of emission color over the entire visible range has emerged as an important task. Similar tasks are met in dye optimization for DSSCs. We discussed in this review issues on DSSCs on the basis of electronic structure and excited states calculations. The main reason for strong phosphorescence in the studied Pt and Ir complexes is connected with the fact that the $S_0 - S_1$ transition moments are relatively low, but the "spin-forbidden" $T_1 - S_0$ transition "borrows" large intensity from the higher lying excited states. This is introduced by SOC at the metal ion, whose electrons are involved in relevant excitations through the metal to ligand charge transfer (MLCT) admixtures. Site-selective phosphorescence in solid matrices at low temperature has revealed that zero-field splitting and spin-sublevel activity can be changed in different sites of the matrix, which shows that the MLCT character of the T_1 state is rather sensitive to the intermolecular environment of the dye. This is an important message; electron-hole recombination also depends on similar factors and all of them should be taken into account in proper simulations of OLEDs.

8. References

Abe, T.; Miyazava, A.; Konno, H. & Kawanishi, Y. (2010). Deuteration isotope effect on nonradiative transition of fac-tris (2-phenylpyridinato) iridium (III) complexes. *Chemical Physics Letters*, Vol. 491, pp. 199-202.

Adachi, C.; Baldo, M.A.; O'Brien, D.F.; Thompson, M.E.; & Forrest, S.R. (2001). Nearly 100% internal phosphorescence efficiency in an organic light-emitting device. *Journal of Applied Physics*, Vol. 90, pp. 5048-5052.

Avilov, I.; Minoofar, P.; Cornil, J. & De Cola, L. (2007). Influence if substituents on the energy and nature of the lowest excited states of heteroleptic phosphorescent Ir(III)

complexes: A joint theoretical and experimental study. *J. Am. Chem. Soc*. Vol. 129, pp. 8247-8258.

Baldo, M.A.; O'Brien, D.F.; Thompson, M.E.; & Forrest, S.R. (1999). Excitonic singlet-triplet ratio in a semiconducting organic thin films. *Physical Review B: Condensed Matter and Material Physics*, Vol. 60, pp. 14422-14428.

Baranoff, E.; Bolink, H. J.; De Angelis, F.; Fantacci, S.; Di Censo, D.;p Djellab, K.; Grätzel, M. & Nazeeruddin, Md. K. (2010) An Inconvenient Influence of Iridium(III) Isomer on OLED Efficiency, *Dalton Transactions*, Vol. 39(2010), pp. 8914-8918, DOI: 10.1039/C0DT00414F.

Baranoff, E.; Fantacci, S.; De Angelis, F.; Zhang, X.; Scopelliti, R.; Gratzrl, M. & Nazeeruddin, M.K. (2011). Cyclometalated Iridium(III) Complexes Based on Phenyl-Imidazole Ligand, *Inorganic Chemistry*, Vol. 50(2011), pp. 451-462, DOI: 10.1021/ic901834v.

Baryshnikov, G.V.; Minaev, B. F. & Minaeva, V. A (2011). Quantum-chemical study of effect of conjugation on structure and spectral properties of C105 sensitizing dye. *Optics and Spectroscopy*, Vol. 110 (3), pp. 393-400.

Barolo, C.; Nazeeruddin, Md. K.; Fantacci, S.; Di Censo, D.; Comte, P.; Liska, P.; Viscardi, G.; Quagliotto, P.; De Angelis, F.; Ito, S.; & Grätzel, M. (2006). Synthesis, Characterization, and DFT-TDDFT Computational Study of a Ruthenium Complex Containing a Functionalized Tetradentate Ligand, *Inorg. Chem.* Vol. 45, pp. 4642-4653.

Bessho, T.; Yoneda, E.; Yum, J.; Guglielmi, M.; Tavernelli, I.; Imai, H.; Rothlisberger, U.; Nazeeruddin, M. K. & Grätzel, M. (2009). New Paradigm in Molecular Engineering of Sensitizers for Solar Cell Applications, *J. Am. Chem. Soc.*, Vol. *131*, pp. 5930–5934.

Bonhôte, P.; Moser J. E.; Humphry-Baker, R.; Vlachopoulos, N.; Zakeeruddin, S. M.; Walder, L. & Grätzel, M. (1999). Long-Lived Photoinduced Charge Separation and Redox-Type Photochromism on Mesoporous Oxide Films Sensitized by Molecular Dyads, *J. Am. Chem. Soc.,* Vol. 121, pp. 1324-1336.

Buchachenko, A.L. (1976). Chemical nuclear polarization. *Russian Chemical Review*. Vol. 45, pp. 375-392.

Chang, C.-J.; Yang, C.-H.; Chen, K.; Chi, Y.; Shu, C.-F.; Ho, M.-L.; Yeh, Y.-S. & Chou, P.-T. (2007). Color tuning associated with heteroleptic cyclometalated Iu(III) complexes; influence of the ancillary ligand. *Dalton Transactions*. Pp. 1881-1890.

Chen, C.; Chen, J.; Wu, S.; Li, J.; Wu, C.; & Ho, K.; (2008). Multifunctionalized Ruthenium-Based Supersensitizers for Highly Efficient Dye-Sensitized Solar Cells, *Angew. Chem. Int. Ed.*, Vol. 47, pp. 7342-7345.

Chen, C.; Wu, S.; Li, J.; Wu, C.; Chen, J.; & Ho, K.; (2007). A New Route to Enhance the Light-Harvesting Capability of Ruthenium Complexes for Dye-Sensitized Solar Cells, *Adv. Mater.* Vol. *19,* pp. *3888–3891*

Chen, L.; You, H.; Yang, C.; Lyu, Y.Y.; Chang, S.; Kwon, O.; Han, E.; Kim, H.; Kim, M.; Lee, H.J. & Das R.R. (2007). Novel, highly efficient blue-emitting heteroleptic iridium(III) complexes based on fluorinated 1,3,4-oxadiazole: tuning to blue by dithiolate ancillary ligands. *Chemical. Communications*, (13) pp.1352-1354.

Cheng, G.; Li, F.; Duan, Y.; Feng, J.; Liu, S.; Qiu, S.; Lin, D.; Ma, Y. & Li, S.T. (2003). White organic light-emitting devices using a phosphorescent sensitizer. *Applied Physics Letters*, Vol. 82, pp. 4224-4226.

Chou, P.T. & Chi, Y. (2007). Phosphorescent dyes for organic light-emitting diodes. *Chemistry – A European Journal*, Vol. 13(2) pp. 380-395.

Cundari, T.R. & Stevens, W.J. (1993). Effective core potential basis sets. *J. Chem. Physics*, Vol. 98, pp. 5555-5565.

De Angelis F., Fantacci S., Evans N., et al. (2007). Controlling phosphorescence color and quantum yields in cationic iridium complexes: a combined experimental and theoretical study. *Inorganic Chemistry*, 46(15) p5989-6001.

Deaton, J.C.; Young, R.H.; Lenhard, J.R.; Rajeswaran, M. & Huo, S. (2010). Photophysical Properties of the Series fac- and mer-(1-Phenylisoquinolinato-N((sect))C(2'))(x)(2-phenylpyridinato-N((sect))C(2'))(3-x)Iridium(III) (x = 1-3). *Inorganic Chemistry*, Vol. 49(20) pp. 9151-9161.

Dedeian K, Shi J, Forsythe E, et al. (2007). Blue phosphorescence from mixed cyano-isocyanide cyclometalated iridium(III) complexes. *Inorganic Chemistry*, Vol. 46(5) pp. 1603-1611.

Forrest, S.R. (2004). The path to ubiquitous and low-cost organic electronic appliances on plastic. *Nature*, Vol. 428, pp. 911.

Gao, F.; Cheng, Y.; Yu, Q.; Liu, S.; Shi, D.; Li, Y. & Wang P. (2008). Ruthenium Sensitizers for High Performance Dye-Sensitized Solar Cells, *Inorg. Chem.* Vol. 48 (6) pp. 2664-2669.

Gao, F.; Wang, Y.; Shi, D.; Zhang, J.; Wang, M.; Jing, X.; Humphry-Baker, R.; Wang, P.; Zakeeruddin, S. M. & Grätzel, M.; (2008). Enhance the Optical Absorptivity of Nanocrystalline TiO_2 Film with High Molar Extinction Coefficient Ruthenium Sensitizers for High Performance Dye-Sensitized Solar Cells, *J. Am. Chem. Soc.*, Vol. 130, pp. 10720-10728.

Haque, S. A.; Handa, S.; Peter, K.; Palomares, E.; Thelakkat, M. & Durrant, J. R. (2005). Supermolecular Control of Charge Transfer in Dye-Sensitized Nanocrystalline TiO2 Films: Towards a Quantitative Structure–Function Relationship, *Angew. Chem. Int. Ed.*, Vol. 44, pp. 5740-5744.

Hayashi, H. & Sakaguchi, Y. (2005). Magnetic field effects and CIDEP due to the d-type triplet mechanism in intra-molecular reactions. *Journal of Photochemistry and Photobiology, C*, Vol. 6, pp. 25-36.

Hirata, N.; Lagref, J.-J.; Palomares, E. J.; Durrant, J. R.; Nazeeruddin, Md. K.; Grätzel, M. & Di Censo, D. (2004). Supramolecular Control of Charge-Transfer Dynamics on Dye-sensitized Nanocrystalline TiO2 Films, *Chem. Eur. J.*, Vol. 10, pp. 595-602.

Hofbeck, T. & Yersin, H. (2010). The triplet state of fac-Ir(ppy)₃. *Inorganic Chemistry*, Vol. 49(12) pp. 9290-9299.

Jansson, E.; Minaev, B.; Schrader, S. & Ågren, H. (2007). Time-dependent density functional calculations of phosphorescence parameters for fac-tris(2-phenylpyridine) iridium. *Chemical Physics*, Vol. 333, pp. 157-167.

Jin, Z.; Masuda, H.; Yamanaka, N.; Minami, M.; Nakamura, T. & Nishikitani, Y. (2009). Efficient Electron Transfer Ruthenium Sensitizers for Dye-Sensitized Solar Cells, *J. Phys. Chem. C* Vol. *113*, pp. 2618–2623.

Karthikeyan, C. S.; Wietasch, H. & Thelakkat, M. (2007). Highly Efficient Solid-State Dye-Sensitized TiO2 Solar Cells Using Donor-Antenna Dyes Capable of Multistep Charge-Transfer Cascades, *Adv. Mater.*, Vol. 19, pp. 1091.

Koseki, S.; Schmidt, M.W. & Gordon, M.S. (1998). Effective nuclear charges for the first-through third-row transition metal elements in spin-orbit calculations. *Journal of Physical Chemistry, A*, Vol. 102, pp. 10430-10435.

Koseki, S.; Fedorov, D.G.; Schmidt, M.W. & Gordon, M.S. (2001). Spin-orbit splittings in the through third-row transition elements: comparison of effective nuclear charge and full Breit-Pauli calculations. *Journal of Physical Chemistry, A*, Vol. 105, pp. 8262-8268.

Kuang, D.; Ito, S.; Wenger, B.; Klein, C.; Moser, J.; Humphry-Baker, R.; Zakeeruddin, S. M. & Grätzel, M. (2006). High Molar Extinction Coefficient Heteroleptic Ruthenium Complexes for Thin Film Dye-Sensitized Solar Cells, *J. Am. Chem. Soc.*, Vol. 128, pp. 4146-4154.

Köhler, A. & Bässler, H. (2009). Triplet states in organic semiconductors. *Material Scienece and Engineering R*, Vol. 66, pp. 71-109.

Köhler, A.; Wittmann, H.F.; Friend, R.H.; Khan, M.S. & Lewis, J. (1994). Organic solar cell based on triplet excitons. *Synthetic Metal*s, Vol. 67, pp. 245-248.

Köhler, A.; Wittmann, H.F.; Friend, R.H.; Khan, M.S. & Lewis, J. (1996). Organic solar cell based on triplet excitons in a bulk heterojunction. *Synthetic Metals*, Vol. 77, pp. 147-150.

Ladouceur, S.; Fortin, D. & Zysman-Colman, E. (2010). Role of Substitution on the Photophysical Properties of 5,5'-Diaryl-2,2'-bipyridine (bpy*) in [Ir(ppy)(2)(bpy*)]PF(6) Complexes: A Combined Experimental and Theoretical Study. *Inorganic Chemistry*, 49(12) p5625-5641.

Lee S.C., Seo J.H., Kim Y.K. & Kim Y.S. (2009). Studies of efficient heteroleptic Ir(III) complexes containing tpy and dfppy ligands for phosphorescent organic light-emitting devices. *Journal Nanoscience Nanotechnology,*Vol. 9(12), pp. 7094-7098.

Li, Y.; Cao, L.; Ning, Z.; Huang, Z.; Cao, Y. & Tian, H. (2007). Soluble porphyrin-bisindolylmaleimides dyad and pentamer as saturated red luminescent materials. *Tetrahedron Letters*, Vol. 48, pp. 975-978.

Li, X.; Zhang Q.; Tu, Y.; Ågren, H. & Tian, H. (2010). Modulation of iridium(III) phosphorescence via photochromic ligands: a density functional theory study. *Phys. Chem. Chem. Phys.* Vol. 12(41) pp. 13730-1376.

Li, X.; Minaev, B.; Ågren, H. & Tian, H. (2011). Theoretical study of phosphorescence of iridium complexes with fluorine-substituted phenylpyridine ligands. *Eur. J. Inorg. Chem.* DOI: 10.1002/ejic.201100084.

Lindgren, M.; Minaev, B.; Glimsdal, E.; Vestberg, R.; Westlund, R. & Malmstrom, E. (2007). Electronic states and phosphorescence of dendron functionalized platinum(II) acetylides. *Journal of Luminescence*, Vol. 124, pp. 302-310.

Liu T., Zhang H.X. & Shu X. (2007). Theoretical studies on structures and spectroscopic properties of a series of novel mixed-ligand Ir(III) complexes [Ir(Mebib)(ppy)X]. *Dalton Transactions*. pp.1922-1928.

Liu, T.; Zhang, H.X. & Xia, B.H. (2007a). Theoretical studies on structures and spectroscopic properties of a series of novel cationic [trans-$(C/N)_2Ir(PH_3)_2$]$^+$ (C/N = ppy, bzq, ppz, dfppy). *J. Phys. Chem. A*, Vol. 111(35) pp. 8724-8730.

Liu, Z.; Nie, D.; Bian, Z.; Chen, F.; Lou, B.; Bian, J. & Huang, C. (2008). Photophysical properties of heteroleptic iridium complexes containing carbazole-functionalized beta-diketonates. *ChemPhysChem*, 2008, 9(4) p634-640.

Minaev, B.F. & Terpugova, A.F. (1969). Spin-orbit interaction in charge-transfer complexes. *Journal of Soviet Physics*, No. 10, pp. 30-36.

Minaev, B.F. (1978). Spin-orbit interaction in molecules and mechanism of the external magnetic field on luminescence. *Optics and Spectroscopy*, Vol. 44, No. 2, pp. 256-260.

Minaev, B.F. (1972). Spin-orbit interaction in doublet states of molecules. *Optics and Spectroscopy*, Vol. 32, No. 1, pp. 22-27.

Minaev, B.; Minaeva, V.; & Ågren, H. (2009). Theoretical Study of the Cyclometalated Iridium(III) Complexes Used as Chromophores for Organic Light-Emitting Diodes. *J. Phys. Chem. A*. Vol. 113, pp. 726-735.

Minaev, B.; Ågren, H. & De Angelis, F. (2009a). Theoretical design of phosphorescence parameters for organic electro-luminescence devices based on iridium complexes. *Chemical Physics*, Vol. 358, pp. 245-257.

Minaev, B.; Jansson, E. & Lindgren, M. (2006). Application of density functional theory for studies of excited states and phosphorescence of platinum(II) acetylides. *J. Chem. Physics*, Vol. 125, pp. 094306-094313.

Minaev, B. & Ågren, H. (2005). Theoretical DFT study of phosphorescence from porphyrins. *Chem. Physics,* Vol. 315, pp. 215-239.

Minaev, B. & Ågren, H. (1999). Spin uncoupling in molecular hydrogen activation by platinum clusters. *J. Molecular Catalysis, A: Chemical*, Vol. 149, pp. 179-195.

Minaev, B.; Wang, Y.H.; Wang, C.K.; Luo, Y. & Ågren, H. (2005). Density functional study of vibronic structure of the first absorption Qx band in free-base porphin. *Spectrochimica Acta, A.* Vol. 65, pp. 308-323.

Minaev, B.F.; Jansson E.; Ågren, H. & Schrader, S. (2006). Theoretical study of phosphorescence in dye doped light emitting diods. *J. Chem. Physics*, Vol. 125, No. 23, pp. 234704.

Minaev, B.F.; Minaeva, V.O.; Baryshnikov, G.V.; Girtu, M. & Ågren, H. (2009b). Theoretical study of vibration spectra of sensitizing dyes for photoelectrical converters based on ruthenium (II) and iridium (III) complexes *Rus. J. Appl. Chem.* Vol. 82, pp.. 1211–1221.

Nazeeruddin, Md. K.; Kay, A.; Rodicio, I.; Humpbry-Baker, R.; Miiller, E.; Liska, P.; Vlachopoulos, N. & Grätzel, M. (1993). Conversion of light to electricity by cis-X2bis(2,2'-bipyridyl-4,4'-dicarboxylate)ruthenium(II) charge-transfer sensitizers (X = Cl⁻, Br⁻, I⁻, CN⁻, and SCN⁻) on nanocrystalline titanium dioxide electrodes, *J. Am. Chem. Soc.*, Vol. 115, pp. 6382-6390.

Nazeeruddin, M.K.; Klein, C.; Grätzel, M.; Zuppiroli, L. & Berner, D. (2009). Molecular engineering of iridium complexes and their application in OLED. In: *Highly Efficient OLED with Phosphorescent Materials*. Yersin, H. ed.Wiley-VCH Verlag GmbH & Co. KGaA, Weinheim.

Nazeeruddin, M. K.; Péchy, P.; Renouard, T.; Zakeeruddin, S. M.; Humphry-Baker, R.; Comte, P.; Liska, P.; Cevey, L.; Costa, E.; Shklover, V.; Spiccia, L.; Deacon, G. B.; Bignozzi, C. A. & Grätzel, M. (2001). Engineering of Efficient Panchromatic Sensitizers for Nanocrystalline TiO$_2$-Based Solar Cells, *J. Am. Chem. Soc.* Vol. 123, pp. 1613-1624.

Ning, Z.; Chen, Z.; Zhang, Q.; Yan, Y.; Qian, S.; Cao, Y. & Tian, H. (2007). *Aggregation-induced emission (AIE)-active starburst triarylamine fluorophores as potential non-doped red emitter for organic light-emitting diodes and Cl$_2$ gas chemodosimeter. Adv. Funct. Mater.* Vol. 17, pp. 3799-3805.

Ning, Z.; Fu, Y. & Tian, H. (2010) Improvement of dye-sensitized solar cells: what we know and what we need to know. *Energy Environ. Sci.,* Vol. 3, pp. 1170-1181.

Ning, Z. & Tian, H. (2009) Triarylamine: a promising core unit for efficient photovoltaic materials, *Chem. Commun.,* Vol. 37, pp. 5483-5495.

Ning, Z.; Zhang, Q.; Wu, W. & Tian, H. (2009a) Novel iridium complex with carboxyl pyridyl ligand for dye-sensitized solar cells: High fluorescence intensity, high electron injection efficiency? *J. Organomet. Chem.,* Vol. 694, pp. 2705-2711.

Ning, Z.; Zhou, Y.; Zhang, Q.; Zhang, J. & Tian, H. (2007a). *Bisindolylmaleimide derivatives as non-doped red organic light-emitting materials. J. Photochem. Photobio. A: Chemistry*, 192, pp. 8-13.

Nozaki, K. (2006). Theoretical study of the triplet state of fac-Ir(ppy)$_3$. *J. Chin. Chemical Society*, Vol. 53, pp. 101-112.

O'Regan, B. C. & Durrant, J. R. (2009) Kinetic and Energetic Paradigms for Dye-Sensitized Solar Cells: Moving from the Ideal to the Real, *Acc. Chem. Res.*, Vol. 42, pp. 1799-1808.

O'Regan, B. & Grätzel, M. (1991) A low-cost, high-efficiency solar cell based on dye-sensitized colloidal TiO$_2$ films, *Nature,* Vol. 353, pp. 737-740.

O'Regan, B. C.; Walley, K.; Juozapavicius, M.; Anderson, A.; Matar, F.; Ghaddar, T.; Zakeeruddin, S. M.; Klein, C. & Durrant, J. R. (2009a) Structure/Function Relationships in Dyes for Solar Energy Conversion: A Two-Atom Change in Dye Structure and the Mechanism for Its Effect on Cell Voltage, *J. Am. Chem. Soc.,* Vol. 131, pp. 3541-3548.

Pope, M.; Kallmann, H.P. & Maganate, P. (1963). *J. Chem. Physics*, Vol. 38, pp. 2042-2050.

Pope, M. & Swenberg, C.E. (1999). Electronic Processes in Organic Crystals and Polymers. *Oxford University Press*, Oxford.

Rausch, A.F.; Thompson, M.E. & Yersin, H. (2009). Blue light emitting Ir(III) compounds for OLEDs - new insights into ancillary ligand effects on the emitting triplet state. *J. Phys. Chem. A.*, Vol. 113(20) pp. 5927-5932.

Rausch, A.F.; Homeier, H.H. & Yersin, H. (2010). Organometalic Pt(II) and Ir(III) triplet emitters for OLED applications. *Topics Orgnometal Chemistry*, Vol. 29, pp. 193-235.

Reynal, A.; Forneli, A.; Martinez-Ferrero, E.; Sánchez-Díaz, A.; Vidal-Ferran, A.; O'Regan, B. C. & Palomares, E. (2008) Interfacial Charge Recombination Between e$^-$–TiO$_2$ and the I$^-$/I$_3^-$ Electrolyte in Ruthenium Heteroleptic Complexes: Dye Molecular Structure–Open Circuit Voltage Relationship, *J. Am. Chem. Soc.* Vol. 130, pp. 13558-13567.

Salikhov, K.M.; Molin, Y.N.; Sagdeev, R.A. & Buchachenko, A.L. (1984). *Spin Polarization and Magnetic Effects in Radical Reactions*, Elsevier, Amsterdam.

Schmidt-Mende, L.; Kroeze, J. E.; Durrant, J. R.; Nazeeruddin, Md. K. & Grätzel, M. (2005) Effect of Hydrocarbon Chain Length of Amphiphilic Ruthenium Dyes on Solid-State Dye-Sensitized Photovoltaics, *Nano. Lett.* Vol. 5, pp. 1315-1320.

Serebrennikov, Y.A. & Minaev, B.F. (1987). Magnetic field effects due to spin-orbit coupling in transient intermediates. *Chemical Physics*, Vol. 114, pp. 359-367.

Snaith, H. J.; Moule, A. J.; Klein, C.; Meerholz, K.; Friend, R. H. & Grätzel, M. (2007) Efficiency Enhancements in Solid-State Hybrid Solar Cells via Reduced Charge Recombination and Increased Light Capture, *Nano. Lett.* Vol. 7, pp. 3372-3376.

Takizawa S.Y., Nishida J., Tsuzuki T., Tokito S. & Yamashita Y. (2007). Phosphorescent iridium complexes based on 2-phenylimidazo[1,2-a]pyridine ligands: tuning of emission color toward the blue region and application to polymer light-emitting devices. *Inorganic Chemistry*, Vol. 46(10) pp. 4308-4319.

Tan, W.; Zhang, Q.; Zhang J. & Tian, H. (2009). Near-Infrared Photochromic Diarylethene Iridium (III) Complex. *Org. Lett.*, Vol. 11, pp. 161–164.

Tang, C.W. & VanSylke, S.A. (1987). Organic electroluminescent diodes. *Applied Phys. Letters*, Vol. 51, No. 11, pp. 913-915.

Vahtras, O.; Lobods, O.; Minaev, B.: Ågren, H. & Ruud, K. (2002). Ab initio calculations of zero-field splitting parameters. *Chemical Physics*, Vol. 279, pp. 133-142.

Volpi G.; Garino C.; Salassa L.; Fiedler J.; Hardcastle K.I.; Gobetto R. & Nervi C. (2009). Cationic heteroleptic cyclometalated iridium complexes with 1-pyridylimidazo[1,5-alpha]pyridine ligands: exploitation of an efficient intersystem crossing. *Chem. Eur. J.* Vol. 15, pp. 6415-6427.

Wong, W.Y. (2008). Metallopolyyne polymers as new functional materials for photovoltaic and solar cell applications. *Macromolecular Chemistry and Physics*, Vol. 209, pp. 14-24.

Wu, Q.-X.; Shi, L.-L.; Zhao, S.-S.; Wu, S.-X.; Liao, Y & Su, Z.-H. (2010). Theoretical studies on photophysical properties of the 2-phenylpyridine iridium (III) complex and its derivatives. *Chem. Journal Chinese Universities*, Vol. 31, pp. 777-781.

Xie, J.; Ning, Z. & Tian, H. (2005). A soluble 5-carbazolium-8-hydroxyquinoline Al(III) complex as a dipolar luminescent material. *Tetrahedron Letters*, Vol. 46, pp. 8559-8562.

Xu, B. & Yan, B. (2007). Photophysical properties of novel lanthanide (Tb^{3+}, Dy^{3+}, Eu^{3+}) complexes with long chain para-carboxyphenol ester p-L-benzoate (L=dodecanoyloxy, myristoyloxy, palmitoyloxy and stearoyloxy). *Spectrochim. Acta A: Mol. Biomol. Spectrosc*. Vol. 66(2) pp. 236-242.

Yang L.; Okuda F.; Kobayashi K.; Nozaki K.; Tanabe Y.; Ishii Y. & Haga M.A. (2008). Syntheses and phosphorescent properties of blue emissive iridium complexes with tridentate pyrazolyl ligands. *Inorg. Chem*. Vol. 47(16) p. 7154-7165.

Yersin, H. & Finkenzeller, W.J. (2008). Triplet emitters for OLED: Basic properties. In: *Highly Efficient OLED with Phosphorescent Materials*. Yersin, H. ed.Wiley-VCH Verlag GmbH & Co. KGaA, Weinheim.

Zapata F.; Caballero A. & Espinosa A. (2009). A redox-fluorescent molecular switch based on a heterobimetallic Ir(III) complex with a ferrocenyl azaheterocycle as ancillary ligand. *Dalton Transactions*, pp. 3900-3902.

Zeng, X.; Tavasli, M. & Perepichka, I.F. (2008). Cationic bis-cyclometallated iridium(III) phenanthroline complexes with pendant fluorenyl substituents: synthesis, redox, photophysical properties and light-emitting cells. *Chemistry – A European Journal*, Vol. 14, pp. 933-943.

Ågren, H.; Vahtras, O. & Minaev, B. (1996). Response theory and calculations of spin-orbit coupling phenomena in molecules. *Advances Quantum Chemistry*, Vol. 27, pp. 71-162.
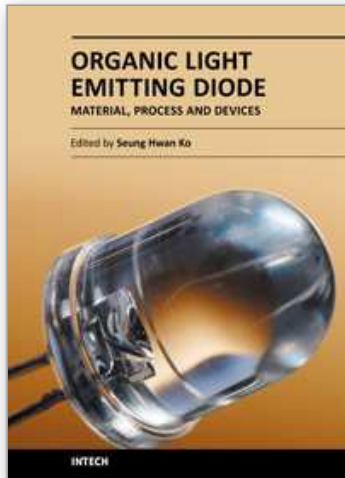
Organic Light Emitting Diode - Material, Process and Devices

Edited by Prof. Seung Hwan Ko

This book contains a collection of latest research developments on Organic light emitting diodes (OLED). It is a promising new research area that has received a lot of attention in recent years. Here you will find interesting reports on cutting-edge science and technology related to materials, fabrication processes, and real device applications of OLEDs. I hope that the book will lead to systematization of OLED study, creation of new research field and further promotion of OLED technology for the bright future of our society.

How to reference

In order to correctly reference this scholarly work, feel free to copy and paste the following:

Boris Minaev, Hans Agren, He Tian, Zhijun Ning and Xin Li (2011). Organometallic Materials for Electroluminescent and Photovoltaic Devices, Organic Light Emitting Diode - Material, Process and Devices, Prof. Seung Hwan Ko (Ed.), ISBN: 978-953-307-273-9, InTech, Available from: http://www.intechopen.com/books/organic-light-emitting-diode-material-process-and-devices/organometallic-materials-for-electroluminescent-and-photovoltaic-devices

INTECH
open science | open minds